

CHALMERS



Finite Element Modelling of Eddy Current Non-Destructive Evaluation in Probability of Detection Studies

ANDERS ROSELL

Department of Applied Mechanics
CHALMERS UNIVERSITY OF TECHNOLOGY
Göteborg, Sweden 2012

THESIS FOR THE DEGREE OF LICENTIATE OF ENGINEERING IN SOLID AND
STRUCTURAL MECHANICS

Finite Element Modelling of Eddy Current Non-Destructive
Evaluation in Probability of Detection Studies

ANDERS ROSELL

Department of Applied Mechanics
CHALMERS UNIVERSITY OF TECHNOLOGY

Göteborg, Sweden 2012

Finite Element Modelling of Eddy Current Non-Destructive Evaluation in Probability of
Detection Studies
ANDERS ROSELL

© ANDERS ROSELL, 2012

Thesis for the degree of Licentiate of Engineering 2012:07
ISSN 1652-8565
Department of Applied Mechanics
Chalmers University of Technology
SE-412 96 Göteborg
Sweden
Telephone: +46 (0)31-772 1000

Chalmers Reproservice
Göteborg, Sweden 2012

Finite Element Modelling of Eddy Current Non-Destructive Evaluation in Probability of Detection Studies

Thesis for the degree of Licentiate of Engineering in Solid and Structural Mechanics

ANDERS ROSELL

Department of Applied Mechanics

Chalmers University of Technology

ABSTRACT

The goal of this work has been to evaluate the possibility to use mathematical modelling to characterize the capability and reliability of automated eddy current inspections. The safety in aerospace propulsion is critical. Components that are critical for the operation are therefore designed to withstand material degradation. This is verified through the use of non-destructive evaluation (NDE) methods. The NDE methods are characterized in a statistical manner by probability of detection (POD) assessments. The result will be different when evaluating different materials, geometries, defect types and also by the specified procedure settings. This is in principle leading to a costly and time consuming campaign for every new NDE application. Eddy current evaluation is one of the most applied methods for NDE of aero engine components and is studied within this work. The nature of the method is complex and there is therefore a need for deeper understanding that may be gained from mathematical models. Such models can have several objectives as for example procedure and equipment optimization or understanding of the method capability and reliability. This work focus on the model based estimation of method capability as the method is applied in a realistic and automated procedure. The finite element method is used for prediction of the eddy current interaction with defects. The work has shown that tight fatigue cracks can be modelled together with the variations of a realistic procedure with good accuracy. Bridging electrical contacts between the faces of the fatigue crack can be captured in a finite element model and is important for a relevant description of the flaw. The influencing procedure parameters with their variability can also be included in the mathematical description resulting in a prediction of the POD as a function of defect size. The model based POD approach has the potential to be an important part in characterization of NDE methods applied to evaluate the structural integrity of components in the future.

Three papers are included in this thesis. The first presents the methodology in the set up of a 3D model of eddy current NDE. The second paper concerns the description of the realistic fatigue crack, evaluated in both models and in experiments. The third paper shows a comparison between an experimental and a model based POD assessment.

Keywords: Non-destructive Evaluation, Eddy Current, Finite Element Modelling, Probability of Detection, Model Based Probability of Detection

to Minette, Novalie & Noomi

PREFACE

This work has been carried out between September 2009 and February 2012 within the European collaboration project PICASSO under the FP7 programme. I have worked as an industrial PhD student at Volvo Aero in the group Process Simulation within the department Materials and Processes.

This thesis would not be presented if I hadn't got the opportunity to work close together with a number of persons. I have also got full support and encouragement from my employer Volvo Aero Corporation. This work has been carried at Volvo Aero in Trollhättan, at Production Technology Centre (PTC) in Trollhättan, at Chalmers University of Technology in Göteborg and in my home. The Volvo Aero investment in this research and the funding from the European Commission within the FP7 programme are greatly acknowledged.

First I would like to give warm thanks to a number of colleagues and friends at Volvo Aero Corporation in Trollhättan: Per Henrikson for your support and encouragement during the whole project from application to finalizing the laboratory equipment and discussion of papers and results; Terho Sulkupuro, Johan Sahlin, Patric Nilsson and Peter Fridolf for all fruitful discussions about eddy current, probability of detection, non-destructive evaluation and life in general; My friends at the department of Process Simulation, for encouragement and philosophies shared about all things, you have been an important part of my working environment. My own learning about being an engineer must be totally blamed on my colleagues at the departments Fabrication and Manufacturing Solutions (9634) and Machining, Inspection and NDT (9640). I wish to thank you all for taking such good care of me.

I would like to thank my supervisor Anders Boström at Chalmers University of Technology for his encouragement and continuous support during this project. My co-supervisors Gert Persson and Håkan Wirdelius in the group Advanced Non-destructive Testing at the department of Materials and Manufacturing Technology, I thank you for all discussions and for the patience and support with my ideas during the work. Apart from my co-supervisors at the Advanced NDT group, I would like to acknowledge Lars Hammar for helping me realize my experimental set ups, Kenneth Hamberg for his support in the material laboratory and Peter Hammersberg for sharing his thoughts about statistics. I would also like to thank Lars Larsson and Erik Lindgren for all discussion about research, cooking and the struggle in the work as a PhD student.

Finally I would like to express my sincere gratitude to the people dear to me, my family and relatives, especially Minette who is always there for me. Without you none of this would be possible. My daughters Novalie and Noomi, you are my sunshine.

Anders Rosell
April 2012

THESIS

This thesis consists of an extended summary and the following appended papers:

- Paper A** A. Rosell and G. Persson (2011). “Modelling a Differential Sensor in Eddy Current Non-destructive Evaluation”. In: *Proceedings of the COMSOL Conference*. COMSOL Conference (Stuttgart, Germany). isbn: 978-0-9839688-0-1
- Paper B** A. Rosell and G. Persson (2012a). “Finite Element Modelling of Closed Cracks in Eddy Current Testing”. In: *International Journal of fatigue* 41, pp. 30–38
- Paper C** A. Rosell and G. Persson (2012b). “Comparison of Experimental and Model Based POD in a Simplified Eddy Current Procedure”. In: 18th World Conference on Nondestructive Testing (Durban, South Africa). (Accepted for publication in conference proceedings)

All papers are written with co-author. I have carried out all computations, experimental work and have written the papers. An other contribution related to this work is

L. Larsson and A. Rosell (2011). “The transition matrix method for a 2D eddy current interaction problem”. In: Review of progress in quantitative nondestructive evaluation (Burlington, Vermont). (To be published in conference proceedings)

The extended summary is in turn divided in six chapters. The first is an introduction to the current work. The second is describing eddy current non-destructive evaluation and the important aspects of the method that relate to modelling. The third chapter describes the numerical modelling using finite elements and how this is applied as a tool for prediction of eddy current measurements. This chapter contains also solutions to some typical probe - flaw interactions. The fourth chapter describes the statistical concepts of probability of detection and how this is used in capability estimation of eddy current procedures. The fifth chapter summarizes the contributions in the appended papers. The final chapter of the extended summary presents the main conclusions and the way forward in the field of eddy current modelling.

Contents

Abstract	i
Preface	v
Thesis	vii
List of symbols	xi
List of acronyms	xi

I Extended Summary

1 Introduction	1
1.1 Background and motivation	1
1.2 Scope and approach for the current work	2
2 Eddy Current Non-destructive evaluation	3
2.1 Introduction	3
2.2 General principles	3
2.3 History in short	4
2.4 Probes	4
2.5 The frequency	7
2.6 Material under test	8
2.7 Defects	9
2.8 Procedures	10
2.9 Experimental system	10
3 Numerical modelling using FEM	13
3.1 Calculation of impedance	14
3.2 Modelling in 2D	15
3.3 Modelling in 3D	17
4 Probability of detection	29
4.1 Introduction	29
4.2 Background	29

4.3	Considerations for EC POD	31
4.4	Parametric \hat{a} versus a methodology	31
4.5	Model based POD	36
5	Summaries of appended papers	39
6	Conclusions and future work	40
	References	42

II Appended Papers A–C

List of symbols

Symbol	Quantity	Unit
E	Electric field intensity	[V/m]
H	Magnetic field intensity	[A/m]
D	Electric flux density	[C/m ²]
B	Magnetic flux density	[T]
J	Current density	[A/m ²]
A	Magnetic vector potential	[Tm]
<i>V</i>	Electric potential	[V]
ϵ	Electric permittivity	[F/m]
μ	Magnetic permeability	[H/m]
σ	Electric conductivity	[S/m]
<i>f</i>	Frequency	[s ⁻¹]
ω	Angular frequency	[s ⁻¹]
<i>Z</i>	Impedance	[Ω]
<i>L</i>	Inductance	[H]
<i>R</i>	Resistance	[Ω]
Chapter 4 Probability of detection		
Symbol	Quantity	
μ	Mean	
σ	Standard deviation	
<i>V</i>	Variance	

List of acronyms

NDE	Non-destructive evaluation
EC	Eddy current
GMR	Giant magneto-resistive
EDM	Electrical discharge machining
FPI	Florescent penetrant inspection
FEM	Finite element method
FE	Finite element
DOF	Degrees of freedom
POD	Probability of detection
PFA	Probability of false alarm

Part I
Extended Summary

1 Introduction

Non-destructive evaluation (NDE) is referring to the range of methods, together with their procedures, that are used to assure the integrity of components and structures without damaging their further use. The methods have in the past relied on the skill and experience of operators. Eddy current (EC) evaluation is one of the most applied methods for NDE. The method is suitable for automated procedures and has the benefit of being environmentally friendly compared to other sometimes interchangeable methods such as fluorescent penetrant inspection (FPI). As the nature of the method is complex, there is a need for a deeper understanding that may be gained from mathematical models. Such models give the possibilities to understand, optimize and also quantify the capability and reliability of the method.

1.1 Background and motivation

Volvo Aero Corporation is designing and manufacturing a large number of components for use in jet-engines and gas turbines. The design commitment puts demands on the quality assurance of components in a life-cycle perspective. A short summary may set this commitment in the context of development in the field of NDE. The first attempts to fly were conducted more than one hundred years ago. Since then there has been a tremendous development of airborne vehicles that now serve as one of the most important links between people around the globe. It was early identified that aircrafts must put safety first in all aspects. This has become more important as airborne travel has increased over the years. The airplanes used today are one of the most challenging structures that exist. They are optimized for safe operation and efficient use with a constant challenge of lowering the environmental impact. During the first fifty years of aircraft usage, the critical parts of an airplane were designed to withstand the ultimate loads that could appear during operation. This included safety factors, if for example there would be weaknesses in the structural parts. Several accidents during the 50's and 60's showed that fatigue and material degradation must be considered in designing critical components used in the aircrafts (ASIAC 1980; Wanhill 2002). The approach of damage tolerance design was adopted and maintenance and overhaul became even more important (Singh 2000). In order to ensure the structural integrity of components and structures, various NDE techniques are employed. This minimizes the risk of having flaws that may grow beyond critical sizes during operation. The capability of the NDE methods is characterized in a statistical manner. The largest defects that may go undetected are used as input for design of critical components. The characterization of NDE methods is carried out through so-called probability of detection (POD) assessments. The outcome from such assessment is in principle a curve stating the detection probability as a function of defect size. The result will be different when evaluating different methods, components, materials, geometries, defect types and also by the specified procedure settings, for example if inspection is carried out manually or with a high level of automation. This is leading to a costly and time consuming campaign for, in principle, every new NDE application. A large number of set ups has to be used in order to get a good statistical estimate of

the POD. The procedure also includes a large number of real defects. A mathematical description and a methodology of using models for the statistical estimation of POD may significantly reduce the cost and time needed for purely experimental assessments. The model based approach may also allow a thorough analysis of the effect on POD from the parameters of the inspection procedure. This can give an efficient tool for optimization and understanding of inspection procedures. The model based approach may sometimes represent the only possibility to get insight or verify special inspections. This includes for example if the desired defects are difficult to retrieve in order to carry out a valid experimental POD estimation. The demands of light weight, reliable aero engine components as well as the design responsibility are requiring increased knowledge of the applied inspection methods. Efficient inspection methods and tools for their capability assessments are therefore important in order to achieve a better market position and improve competitiveness.

1.2 Scope and approach for the current work

Numerical modelling of the EC method has been developed since the 60's (Auld and Moulder 1999). It was early shown that such methods could be used to predict flaw response characteristics. The goal here is to continue this development in order to build a model capable of predicting the POD corresponding to a realistic, automated EC procedure. This means to construct a POD curve based on a real procedure but created by a mathematical model of the underlying physical principles. The research question for this work has been:

How can a mathematical model be used to predict the probability of detection for automated eddy current procedures?

This work focuses on procedures for detection of surface-breaking fatigue cracks. The materials considered are nonmagnetic and crack sizes are around one millimetre. The finite element method (FEM) is used for describing the EC method in a mathematical model. This technique represents one of several mathematical techniques for solving the underlying equations which describe the governing physical principles. This choice is based on the possibility to include complex geometries in order to arrive at predications of configurations close to reality. The method allows a more realistic description of the part but may also be one of the few possibilities for modelling of the true, individual flaw. The crack represents a local variation in the material and the model is restricted to the volume of the magnetic field in proximity to the flaw. Models created with a high number of parameters are studied. The goal is to reach a comparison between real and modelled POD assessments in realistic procedures. This involves the understanding of how to model real defects and to include process variations. It was therefore decided at an early stage to use a commercial software package for the three dimensional finite element analysis.

2 Eddy Current Non-destructive evaluation

2.1 Introduction

This chapter serves as a short review of the eddy current method as it is used for NDE. The different aspects described give the framework for modelling of the method and also to POD assessments. The applications studied in this work relates to surface inspection of paramagnetic materials evaluating small (~ 1 mm) surface breaking fatigue cracks. Experimental work with the method is carried out for validation purposes within the work presented. A description of the experimental set up and applied analysis tools are therefore described briefly in this context. Some references are given in the text but for general information it is recommended to consult for example (Udpa and Moore 2004; McMaster et al. 1986; Blitz 1997; Shull 2002; Cecco et al. 1983; Hagemaiier 1990).

2.2 General principles

Eddy current is an electromagnetic method used for non-destructive evaluation of materials. An alternating current (AC) is applied to a conductive element which generates a magnetic field surrounding the eddy current probe. The frequency of the field is usually ranging from a few kHz to several MHz for typical NDE applications. The magnetic field interacts with the material under test, which must have the physical properties that enable changes in the magnetic field that correspond to the variable of interest. The eddy current method evaluates thus only conductive materials even though this also includes low conductivity materials such as graphite-epoxy composites. The magnetic field from the probe is inducing electrical currents (eddy currents) in the test object and the measurement is a description of the state of these. Changes are depending on variations of electric conductivity and permeability in the volume of the magnetic field. The field and thus also the induced currents are decreasing fast into the depth of a conductive material. The method is therefore applied for measurements of properties or detection of defects close to the surface. The response of the applied magnetic field can reveal information of material conditions such as hardness, thickness, presence of corrosion, or defects such as porosity and cracks. The eddy current system measures this response of the material property, which is causing changes in the induced currents, as a variation of probe impedance. The variation is presented, after signal conditioning, on the display of the eddy current instrument. The output impedance must in general be interpreted through the use of a reference, which is an important part of any eddy current measurement. There are several steps of technique optimization which have an impact on the usage and application ranging from the probe to the inspection set up, frequency, the material under test and finally the expected flaw characteristics. Maxwell's equations describe the physical laws behind eddy current NDE. The equations are not given here but are described in textbooks regarding electromagnetic field theory, the formulation for eddy current problems is presented in **Paper B**.

2.3 History in short

Eddy current evaluation has its roots in discoveries made more than 150 years ago. In 1831 both Joseph Henry and Michael Faraday discovered the phenomenon of electromagnetic induction. The principles behind these laws of nature were later explained by James Clerk Maxwell in his formulation of electromagnetic field theory in 1864¹. The first practical eddy current test was conducted by David E. Hughes who in 1879 used the telephone invented three years earlier as a device for producing signals corresponding to the imbalance between two pairs of coils (Hughes 1879). Hughes measured the electrical conductivity of different metals using copper as a reference value. This approach has led to a conductivity unit described by the percentage of this reference in the International Annealed Copper Standard (IACS). Rapid technological developments during World War II demanded non-destructive testing techniques. During this time the modern eddy current equipment was formed by Friedrich Förster. He developed precise theories for many basic eddy current tests and pioneered the impedance plane display in the early 40's (Förster 1983). He developed many specialized solutions and laid the foundation of one of the biggest advantages of eddy current inspection; the precise theoretical descriptions. A more complete list of Förster's contributions are summarized in the first edition of the NDT Handbook (McMaster 1959). The electrical signal handling and instrumentation have gone a long way from the use of impedance plane curves introduced by Förster in the 40's and further, with the microprocessors in the 70's, to now use the capacity of modern computers. This allows every technical application to be customized for its purpose. The development has created possibilities to work with signal processing ranging from filtering and statistical noise reduction to inverse modelling (Auld et al. 1988; Udpa and Udpa 1996) and neural networks (Song and Shin 2000; Ren and Ida 2002). The technique is now allowing the user to tailor the instrument characteristics to the application very effectively. Eddy current is today one of the most employed methods of non-destructive evaluation.

2.4 Probes

Construction of a suitable probe is a procedure that has large impact on understanding the operation principles of the eddy current application. The object under test is in general placed under the probe for inspection on open surfaces (some difference in the discussion holds for tubular, wire or similar inspections). It is therefore desirable to direct the magnetic field towards the surface under the probe. This implies that the current carrying element of the probe usually is wound into a coil and that ferromagnetic materials can be used for shielding the field in the other directions. Ferromagnetic material placed inside the coil will give a focusing effect to the applied field. The ferrite will also enhance the magnetic field strength inside the probe and is widely used in order to increase the signal to noise ratio. A ferromagnetic core may also serve better against wear as the probe

¹The equations are appearing in his four part article *On physical lines of force* published in 1861 and 1862. The original set of equations is first formulated in *A Dynamical theory of the electromagnetic field* in 1864, published 1865. His work on the theory of electromagnetism is finally summarized in the book *A Treatise on Electricity and Magnetism* which was published in 1873.

is scanned over a test object surface, Polytetrafluoroethylene (PTFE) tape is also widely used as a protective and replaceable layer. The copper coil is usually placed inside an epoxy body and the winding has a thin isolating layer for protection of currents flowing between the wound layers of the coil.

The coil that is carrying the external current can also serve as sensor of changes in impedance. In that case called an absolute probe, see figure 2.1. However it is also common to use another coil for sensing or to measure the impedance difference between two or more coils. This can be extended to the construction of array or matrix probes to gain larger coverage in a single scan (Grimberg et al. 2006). Specialized probes may have complex geometries and can also be sensitive to the direction of the scan, for example when optimized for detection of defects below the surface (Stepinski 2002; Uchanin 2001). There are also probes that are developed for specialized inspections, for example welds (Noritaka et al. 2006). The sensing elements, which usually are coils, can be replaced by Hall or giant magneto-resistive (GMR) sensors, especially to get higher sensitivity at low frequencies (Dogaru and Smith 2001). Probes produced as printed circuits are also developing as well as specific assemblies that give possibilities to adapt to curved surfaces (Marchand et al. 2010), or the so-called Meandering Winding Magnetometer (Goldfine and al. 2005). The magnetic field exciter and the receiving element must be included in a mathematical model of the EC inspection, which therefore may need a complex probe description.

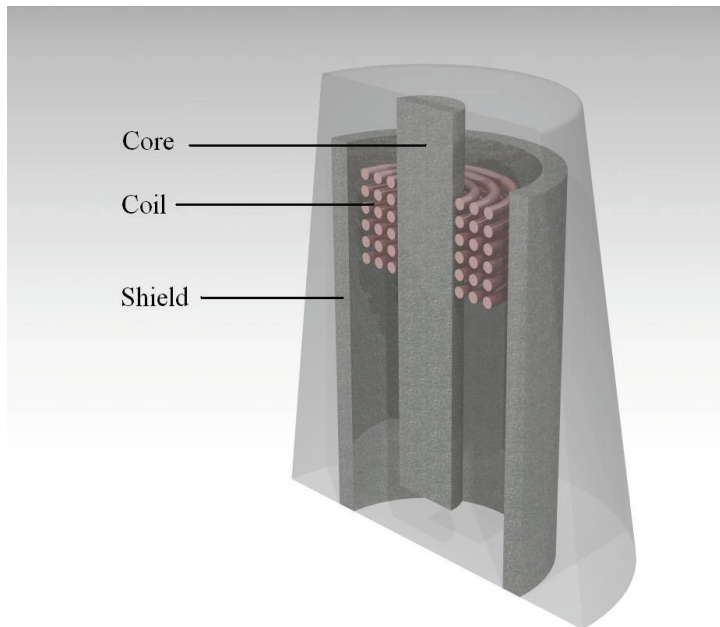


Figure 2.1: *Cross section of an absolute eddy current probe with ferrite core and shielding.*

It is important to ensure a good coupling of the generated magnetic field to the object that is inspected and the volume where defects might occur. The positioning of the probe must be as close to the surface as possible, with an optimal alignment. The distance between the test surface and the probe is referred to as lift-off. This parameter must be kept of the order of 0.1 mm, when the EC method is applied to small cracks, see figure 3.14 on page 26. The tilt angle of the probe i.e. the difference between the probe axis and surface normal has an impact similar to that of lift-off for small angles (Zhang et al. 2008). If the surface of the test object is curved there will be a similar reduction in the coupling of the magnetic field to the object under test. It is important to point out that it is often crucial to keep these variable under control and as constant as possible as the probe is scanned over a surface. Therefore, it is common to put the probe directly on the surface during a scan even if it in principle would be possible to inspect without being in contact with the component. It is common practice to use a spring load on the probe to ensure a constant lift-off against the surface under test. Calibration principles where the probe tilt angle can be adjusted are also used to ensure that the inspection is carried out under optimal conditions regarding the positioning. The variation of sensitivity between probes can be considerable. This must in general be considered in technique capability assessments and evaluated by use of references. The reason for difference between probes can be variations in probe assembly, which often is manual in many stages. The influence on the induced currents arising from some parameters can be evaluated in a mathematical model. Figure 2.2 shows calculations of the induced surface current density from a typical absolute probe. There is also possibilities of using for example photoinductive field mapping to retrieve variations between individual probes experimentally (Moulder and Nakagawa 1992).

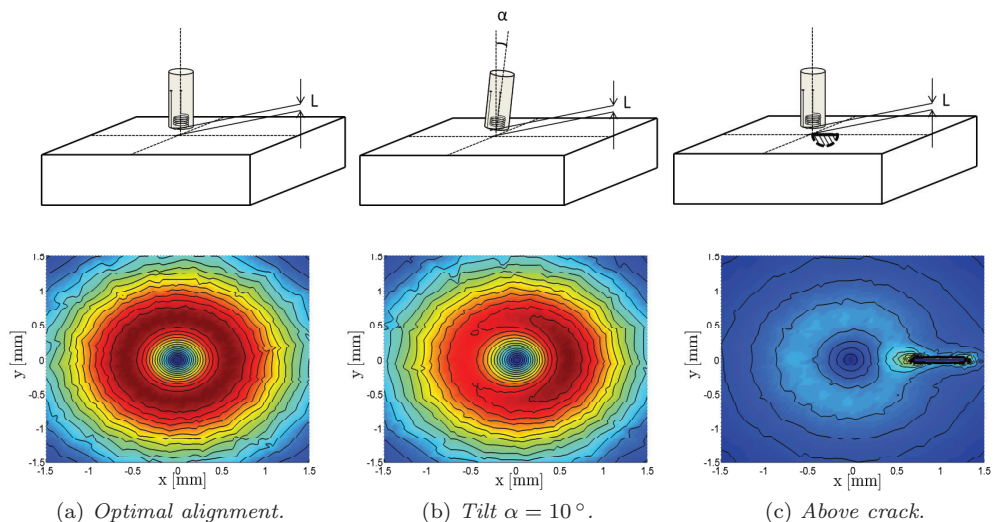


Figure 2.2: *Induced surface current density from an absolute eddy current probe.*

2.5 The frequency

The frequency of the applied alternating current has a correlation to the design of the probe as the impedance is measured close to the resonance frequency of the probe circuit. The probe represents a sensor leg in a bridge-balancing circuit where other parameters are variable for adaption to the specific electrical properties of the probe. However, the frequency of the magnetic field will be the same as that of the current in the coil and the value of this property has a direct impact on the inspection. The impact from frequency shows some important properties from the underlying physics of eddy current. Assume that the magnetic field from the probe can be approximated as a plane wave directed towards a conductive material along the z -axis, $H_x = H_{0x}e^{j(\omega t - kz)}$, where $k = \sqrt{j\omega\mu\sigma - \omega^2\mu\epsilon}$, see for example (Shull 2002) for detailed derivations. If we consider the eddy current application which in general is performed at a single constant frequency on a conductive material, then $\sigma \gg \omega\epsilon$. This states that the displacement currents can be ignored, which is a liable approximation since the conduction currents dominate in the material and the source current in the air region of the eddy current problem (Bossavit 1998). The expression for the induced current density in the conductive material becomes

$$J_y(z) = J_{0y}e^{-(1+j)\sqrt{\frac{\omega\mu\sigma}{2}}z}e^{j\omega t} \quad (2.1)$$

Here, J_{0y} represents the current density at the surface. The result shows that the amplitude of the induced current density decays exponentially into the depth of the material and also that there is a phase lag. This decay of current is described with the penetration depth (often called skin depth in electromagnetics)

$$\delta = \sqrt{\frac{2}{\omega\mu\sigma}} \quad (2.2)$$

The equation describes the depth where the current density is $J_{0y}e^{-1}$ or 37% of J_{0y} and the phase lag 57.3° . The penetration depth is depending on the properties of the material under test as well as the frequency of the applied current of the probe, a parameter that is controllable. The final choice of frequency depends on the properties of the material under test and the desired penetration depth of the applied eddy current inspection. For near surface crack detection purposes it is of the order of the crack depth. The derivations are however based on a plane wave approximation of the magnetic field from the probe and under more realistic conditions the actual depth will be smaller, see for example figure 3.2 on page 18. It is important to bear in mind that the signal strength in a normal eddy current sensor is proportional to the frequency of the magnetic field. This makes inspection more difficult at low frequencies. A practical issue is also that a lower frequency decreases the phase difference between defects and lift-off response. This is displayed in the impedance plot presented in figure 2.3.

The signal from a fatigue crack is included in figure 2.3 as well as calculated trends that results from lift-off, ω and σ changes. The normalized impedance plane is constructed by dividing all values with ωL_0 which represents the impedance of the probe in air. Many turns are used in probe windings for low frequency applications or even other magnetic

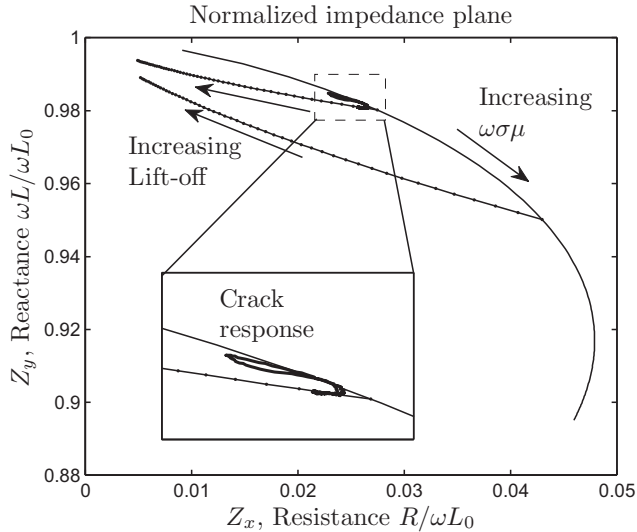


Figure 2.3: *Trend curves in the impedance plane typical for non-magnetic materials.*

sensors such as Hall of GMR as previously mentioned. The frequency should in general be selected to optimize the signal response with respect to the desired flaw and the sensitivity to noise factors.

2.6 Material under test

The derivation of the penetration depth reveals the importance of consideration of the permeability μ and electric conductivity σ . The materials studied within this work are paramagnetic which imply that μ is close to the permeability of free space μ_0 . This is an important limitation of the work as this reduces the physical problem to only consider linear materials in contrast to nonlinear materials which show hysteresis effects. The small magnitude of the magnetic fields associated with eddy current inspection allows, however, good approximation with a constant permeability even for ferromagnetic materials including the ferrite material in the probe (Bossavit 1998). The electric conductivity σ is in most applications a constant material property but can vary significantly for example in coarse grained Titanium alloys (Blodgett et al. 2000). Figure 2.4 presents a surface plot of the measured impedance amplitude over the interface between cast (left) and welded (right) Ti-6AL-4V material. The grain structure in the cast material introduces noise due to inhomogeneous and anisotropic conductivity (Neighbor 1969). In addition to this the conductivity responds to an applied mechanical stress. The material is then showing magneto-resistive characteristics. This has been shown to occur in both Titanium alloys and Nickel-based super alloys (Blodgett and Nagy 2004; Feng et al. 2006). All the possible parameters influencing the magnetic material properties can be a source of noise. An eddy current system may, however, present a solution for evaluation of such parameters.

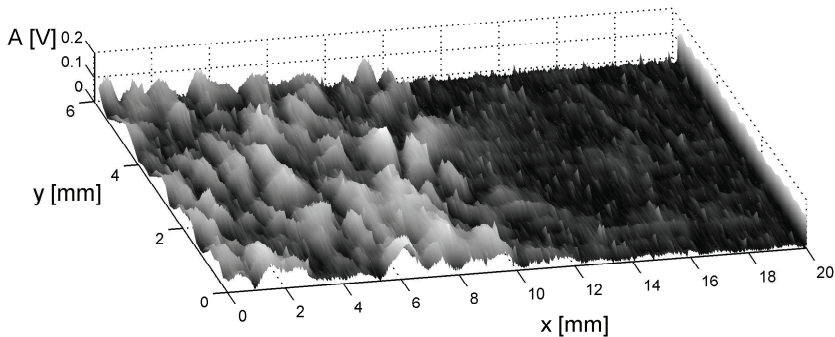


Figure 2.4: *Impedance amplitude as a function of probe coordinate. The variation arise due to conductivity variations in cast (left) and welded (right) Ti-6AL-4V, respectively.*

2.7 Defects

Probability of detection assessments used for aerospace components are often designed according to (MIL-HDBK-1823 2009). The procedures used for eddy current testing require the use of fatigue cracks for capability assessments. These cracks ensure proper capability estimations both for inspection procedures during maintenance and after manufacturing. Cracks used in these assessments are often manufactured in the laboratory in order to achieve a sufficient variation of sizes. Several of the cracks used in this work were broken open and their shape studied, see figure 2.5. The half circular shape and the almost perpendicular alignment against the surface are characteristic properties of these cracks.



Figure 2.5: *Fatigue crack in Ti-6AL-4V.*

The laboratory grown fatigue crack represents a natural crack. However, in eddy current testing it is common to evaluate, calibrate and train from artificial defects (notches) created by electrical discharge machining (EDM). These EDM notches are easy to manufacture in components as references or calibration objects. The width of a small EDM notch is typically $\sim 50 - 100\mu\text{m}$ which is considerably larger compared to a fatigue crack. The notch must thus be treated as an artificial defect and does not in general represent a real defect.

2.8 Procedures

The output from an EC system is a signal describing the measured impedance in the sensing elements of the probe. This signal is usually altered by various processing steps. The probe is often represented as one leg in a balancing bridge circuit (e.g. Wheatstone bridge). The operator can set some of the other parameters to place the signal at zero voltage on flaw-less material in order to optimize the response of defects (or sensitivity to variations from this balancing point). This procedure is called nulling and is handled by the inspection system. The signal may also be amplified, filtered through high-, low- or band pass filters, rotated in phase to finally be displayed on an EC instrument or a connected computer. The evaluation of the integrity of the material must thus be based on the use of references containing a flaw, artificial or real which relate the signal to the state of the object that is inspected. The specific requirements and conditions for an inspection must be considered in the procedure. These must then be transferred to mathematical descriptions if the inspection is to be understood by the use of a model. There is a lot of literature describing how the signal response should be interpreted under various conditions. The interpretations require, in general, highly skilled and experienced operators. To enable a good inspection procedure it is important to ensure

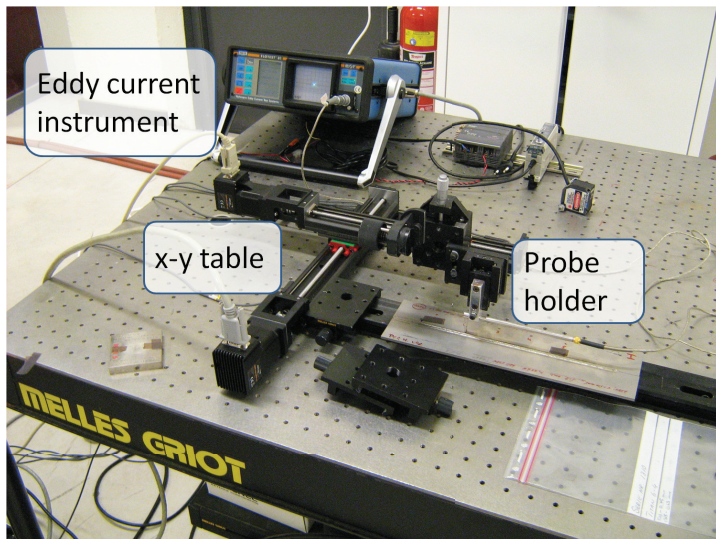
- Coverage of the surface to be inspected
- The sensitivity is sufficient
- Noise parameters are identified and controlled
- The detection capability is verified
- Impedance signals is accurately interpreted
- The system is maintained over time

A physical model describing the system can aid in all the points above and this is the driving force behind model based signal predictions. The first five points are studied through probe-flaw response prediction and model based POD. The last point is aided by theoretical understanding and training of personnel.

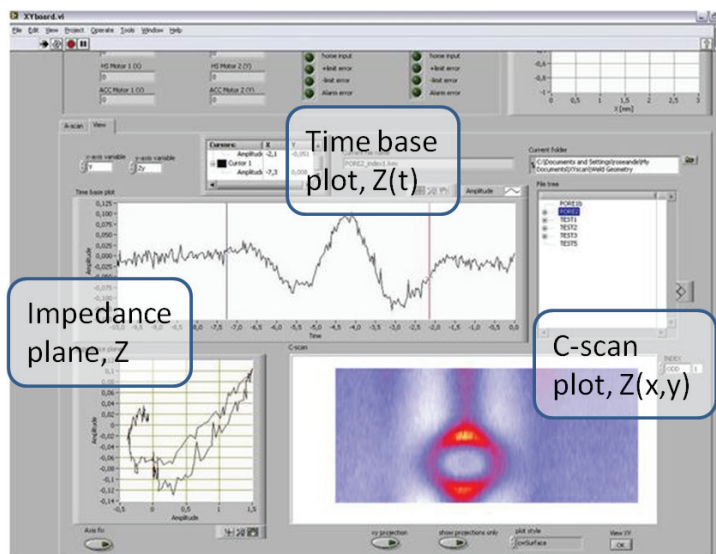
2.9 Experimental system

A laboratory system to carry out EC measurements was built in order to validate the numerical models and the approach for model based POD assessments. The goal of this system was to be able to move different probes in a controlled motion and continuously capture the eddy current output signal together with the position of the probe. The system was set up using two linear guide actuators connected perpendicularly to form an x - y table, see figure 2.6. Two stepper motors were connected to the actuators for movement of the probe holder. A control unit was connected to the motors and a LabVIEW program built in order to control the motion and signal capture. The LabVIEW program was developed to handle the eddy current data and to build signal maps in the x - y plane

using the impedance signal from individual scans, see figure 2.7. A surface scan may take up to 30 minutes capturing x , y and time signals at a sampling rate of 50 Hz, generating signal map image sizes of 1-10 Mb.



(a) x - y table.



(b) Labview control program.

Figure 2.6: Experimental eddy current system.

The experimental system is built to handle different probe types and for x - y scan with high position accuracy of the order of $\sim 10 \mu\text{m}$. The high position accuracy results in a restriction of the scan speed which must be low $\leq 5 \text{ mm/s}$. The probe holder has a micrometer actuator along the z axis and is spring loaded when the probe is put down directly on to the surface. The z positioning is handled manually and decoupled from the motion control system. Using a raster scan with an index step of $50 \mu\text{m}$ gives a detailed signal response map over a surface. This index step is used in figure 2.7. The fatigue crack studied has a length of 1.02 mm . The amplitude is given as a fraction of the response from the calibration notch $|Z_N|$, which in this case is rectangular with dimensions 0.76 mm long, 0.38 mm deep and 0.076 mm wide.

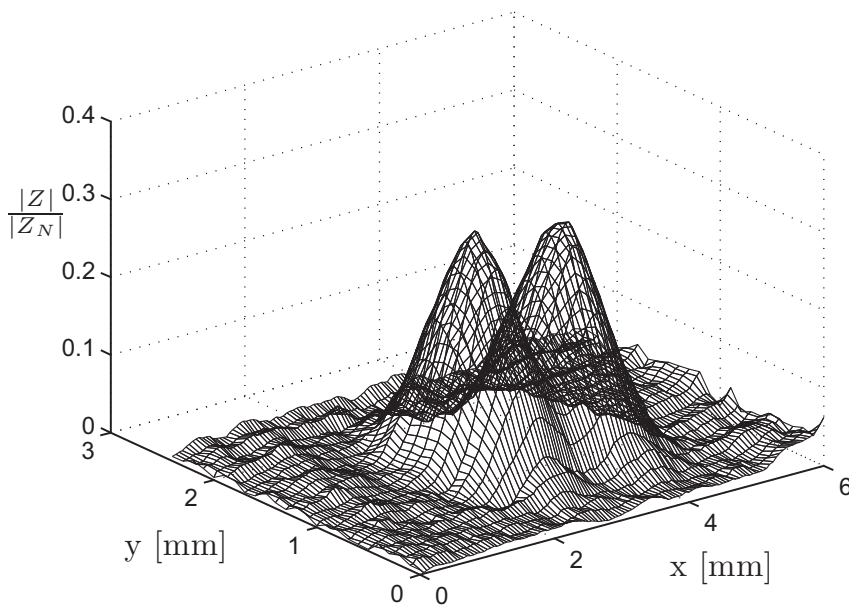


Figure 2.7: Detailed scan over a 1.02 mm long, penny-shaped fatigue crack. The crack is positioned approximately in the point $(3,1)$ and oriented parallel to the x -axis.

3 Numerical modelling using FEM

Förster was among the first to develop analytical tools to explain experimental findings and for predicting the effects of test object properties in eddy current measurements. Concerning analytical methods of modelling eddy current the most important early contribution to the field was made by Dodd and Deeds who in the late 1960's derived integral expressions for the impedance of a coil (Dodd and Deeds 1968). The derivations concerned the impedance of a coil above a layered half-space conducting medium as well as of a finite length coil encircling a conducting rod. These models are still widely used for such geometries, also within this work (**Paper A**) and figure 2.3. One essential feature is the description of the individual windings as a current carrying sheet within the coil, which is a useful and widely accepted approximation.

Finite element modelling of eddy current phenomena started with pioneering work in the 1970's. The first geometries studied were axisymmetrical and showed direct evidence of the usefulness of the method (Palanisamy and Lord 1979; Ida et al. 1983a; Ida et al. 1983b). The magnetic vector potential, \mathbf{A} , is applied for this type of problems due to the fact that Gauss equation $\nabla \cdot \mathbf{B} = 0$ is satisfied automatically. The eddy current problem is convenient to formulate as a low frequency problem which is a natural and accurate description as conduction currents is large compared to displacement currents (Bíró and Preis 1989). There are many textbooks concerning numerical modelling of electromagnetics including eddy currents, one more devoted to NDE applications may be explicitly recommended (Ida 1995). The general description of the formulation using the magnetic vector potential \mathbf{A} and the electric scalar potential V is

$$\nabla \times \left(\frac{1}{\mu} \times \mathbf{A} \right) + \sigma \left(\frac{\partial \mathbf{A}}{\partial t} + \nabla V \right) = \mathbf{J}_s \quad (3.1)$$

$$\nabla \cdot \sigma \left(\frac{\partial \mathbf{A}}{\partial t} + \nabla V \right) = 0 \quad (3.2)$$

$$\nabla \cdot \mathbf{J}_s = 0 \quad (3.3)$$

where \mathbf{J}_s is the external current of the coil, μ the magnetic permeability and σ the electrical conductivity. The magnetic potential is, however, not uniquely determined as any gradient of a scalar potential, ∇V , can be added without changing the magnetic field \mathbf{B} , this is called gauge condition. Using different gauge conditions for the magnetic vector potential in eddy current formulations are studied in (Song and Ida 1991; Morisue 1993). The first 3D FE models used nodal elements (Ida et al. 1985; Bíró and Preis 1990) but later also edge elements. Edge elements give good approximations even at corners where the permeability changes, which is a problem with nodal formulations (Bíró 1999; Liu et al. 2002). The accuracy and computation efficiency is also showed to be improved by edge element formulations (Nakata et al. 1990; Nakata et al. 1991; Preis et al. 2000). Edge elements have basis functions with tangential components that are continuous across element borders but the normal component is allowed to be discontinuous. This is suitable for approximative solutions of curl-curl equations of vector quantities such as the

magnetic vector potential. Developments within the field of finite element analysis have rendered a wide range of commercially available software packages that can be utilized for eddy current related analysis. Edge elements are mainly used together with the software COMSOL Multiphysics for the 3D computations within this work.

3.1 Calculation of impedance

The interesting output variable from a model of an eddy current inspection is the impedance. This is the experimental quantity that is used for the material integrity evaluation. The principles of calculation of impedance from a numerical model are presented below. First, the 2D and the axisymmetrical case are studied, these are very similar. For such problems the electric field and magnetic vector potential are assumed to be constant along one of the coordinate directions. The voltage induced in a length of wire is described according to

$$V = j\omega \int_S \mathbf{A} \cdot d\mathbf{S} \quad (3.4)$$

It is then possible to compute the impedance response in a single loop with radius r , carrying the current I , as $Z = V/I = j\omega 2\pi r A_\varphi(r, z)/I$ in the axisymmetrical case. The single loop describes a delta function coil existing only in the position (r, z) . Superposition of many such delta coils are used to account for the width and height of the more realistic coil. Assuming that the current density is homogeneous within the coil gives the total impedance of the coil by

$$Z = \frac{j\omega 2\pi n^2}{i_0 A_c^2} \iint_{A_c} A(r, z) r \, dr dz \quad (3.5)$$

Here, i_0 is the current density, n is the number of loops and A_c is the total cross-sectional area of the coil. It is assumed that the number of loops per area is constant. The result in equation (3.5) relies on the symmetry of the magnetic vector potential which must be constant along the direction of the electromotive force within the coil. This is not the case in 3D which therefore calls for other alternatives. The calculation of impedance can then be made considering the energy of the system containing the probe, material, defect and surrounding air. The calculation of impedance from energy considerations relies on the use of Poynting's theorem for complex phasors

$$\mathbf{P} = \mathbf{E} \times \mathbf{H}^* \quad (3.6)$$

where $*$ is indicating complex conjugate. Poynting's vector \mathbf{P} is representing the complex power emitted from the input terminals to the electromagnetic fields. The complex notation is suitable since EC problems are treated as quasi-static in time. Using Ohm's law gives the relation between the impedance and the power as $Z = P/I^2$. This allows a relation between the electromagnetic fields and the impedance of the parts carrying

external current. The resulting equation of the impedance due to a defect is

$$\Delta Z = Z_b - Z_a = \frac{1}{I \cdot I^*} \oint_s (\mathbf{E}_b \times \mathbf{H}_b^* - \mathbf{E}_a \times \mathbf{H}_a^*) \cdot \hat{\mathbf{n}} dS = \frac{j\omega}{I^2} \int_V (\mu_b \mathbf{H}_b \cdot \mathbf{H}_b^* - \mu_a \mathbf{H}_a \cdot \mathbf{H}_a^*) - \left(\frac{\sigma_b}{j\omega} \mathbf{E}_b \cdot \mathbf{E}_b^* - \frac{\sigma_a}{j\omega} \mathbf{E}_a \cdot \mathbf{E}_a^* \right) dV \quad (3.7)$$

where Z_b and Z_a represent the impedance with and without the defect respectively. Here, V is the total volume of the model and an accurate calculation of impedance is in some sense relying on a capture of the total field build up by the external current in the coil (Ida 1988).

3.2 Modelling in 2D

A 2D model in plane symmetry was studied and compared to an analytical solution in (Larsson and Rosell 2011). The FEM model was implemented in MATLAB following the principles in (Bondeson et al. 2005). This implementation is described here in order to present a simplified (as being 2D) FEM implementation of the eddy current problem using first order nodal elements. The 2D problem with currents flowing in the z -direction has variations occurring only in the x - and y -directions. The potentials \mathbf{A} and V can be chosen as

$$\mathbf{A} = A_z(x, y)\hat{\mathbf{z}}, \quad V = 0 \quad (3.8)$$

The electric potential is constant over the whole cross sectional area as no driving force can create currents other than in the direction out of the plane. Writing the magnetic field $\mathbf{B} = \nabla \times \mathbf{A} = \nabla A_z \times \hat{\mathbf{z}}$ gives, based on equations (3.1)–(3.3), the final equation

$$-\nabla \cdot \mu^{-1} \nabla A_z + j\omega \sigma A_z = J_z^s \quad (3.9)$$

The solution of A_z must be restricted to a limited domain S in space. The outer boundary is situated far from any source current which corresponds to setting $A_z = 0$ on ∂S . The truncation of outer boundaries must be set sufficiently far away from the probe (**Paper A**). This problem is shared in many open boundary electromagnetic problems and other treatments using hybrid models (Nath et al. 1993; Fetzner et al. 1997) or so-called infinite elements have been considered (Ida et al. 1987). Multiplying equation (3.9) with a test function $w^{(i)}$ and integrate over the total surface S gives

$$\int_S \mu^{-1} \nabla w^{(i)} \cdot \nabla A_z + j\omega \sigma w^{(i)} A_z dS - \underbrace{\int_{\partial S} w^{(i)} \mu^{-1} \nabla A_z dL}_{\text{set } w^{(i)}=0 \text{ on } \partial S} = \int w^{(i)} J_z^s dS \quad (3.10)$$

Expanding the magnetic vector potential in a set of basis functions gives

$$A_z(x, y) = \sum_{j=1}^N A^{(j)} \varphi^{(j)}(x, y) \quad (3.11)$$

where N is the total number of basis functions used in the expansion. The number of these basis functions corresponds to the nodes of the triangular mesh. Usage of Galerkin's method, i.e. $w^{(i)}(x, y) = \varphi^{(i)}(x, y)$ for all nodes where A_z is unknown and substituting (3.11) into (3.10) gives a linear system of equations, $\mathbf{A}\mathbf{z} = \mathbf{b}$. The coefficients are given by

$$A^{(ij)} = \int_S \mu^{-1} \nabla \varphi^{(i)} \cdot \nabla \varphi^{(j)} + j\omega\sigma\varphi^{(i)}\varphi^{(j)} dS \quad (3.12)$$

$$z^{(j)} = A_z^{(j)} \quad (3.13)$$

$$b^{(i)} = \int_S \varphi^{(i)} J_z^s dS \quad (3.14)$$

Implementation of a linear basis function is used here. The basis functions have the value of 1 for node i and zero on the other nodes of an element.

$$\varphi^{(i)} = a^{(i)} + b^{(i)}x + c^{(i)}y. \quad (3.15)$$

The matrix and vector components (3.12)–(3.14) are computed by considering the contribution from each element. The coefficients are computed as

$$A^{(ij)} = \int_S \mu^{-1} \nabla \varphi^{(i)} \cdot \nabla \varphi^{(j)} + j\omega\sigma\varphi^{(i)}\varphi^{(j)} dS \quad (3.16)$$

$$= \sum_{e=1}^E \int_{S_e} \mu^{-1} \nabla \varphi^{(i)} \cdot \nabla \varphi^{(j)} + j\omega\sigma\varphi^{(i)}\varphi^{(j)} dS_e \quad (3.17)$$

where E is the number of elements and S_e is the element surface. The conductor is assumed to be built up from a homogeneous distribution of current carrying wires. The individual current in each wire is I and a total number of wires are n . The wire structure is difficult to maintain in a simple finite element analysis, so an evenly distributed current over the cross-sectional area of the conductor is assumed. The external current applied to node i is then described as

$$b^{(i)} = \sum_{e_i} \frac{1}{3} \frac{A^{(e_i)}}{A_C} \cdot I n \quad (3.18)$$

where the sum is taken over the elements e_i with area $A^{(e_i)}$, carrying the external current and connected to node i . A_C in equation (3.18) is representing the cross-section area of the conductor. A comparison with an analytical approach is presented in (Larsson and Rosell 2011). The geometry studied is a straight conductor carrying external current over a conductive half plane with a cylindrical defect. Comparison with the derived analytical solution can be useful when setting up and understanding the FE model. Figure 3.1 shows the impact of element size at various frequencies. This is corresponding to different depths of penetration of the induced currents. The result is important to consider in 3D models in order to get accurate results with a limited number of degrees of freedom (DOF). The figure shows that the penetration depth must be resolved with approximately four linear elements in order to give sufficient accuracy in signal prediction.

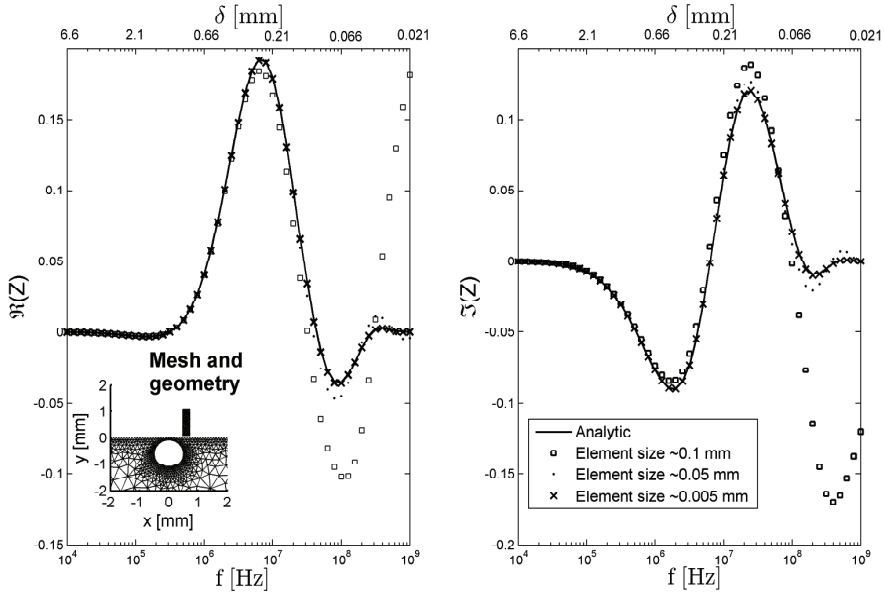


Figure 3.1: *Real and imaginary part of the impedance as a function of frequency. Different mesh densities are compared to an analytic solution. Mesh presented around the flaw of the 2D problem and element size at the surface stated.*

3.3 Modelling in 3D

One of the great benefits of FEM is that general geometries can be studied. In modelling of EC NDE this feature enables the study of signal responses on curved surfaces as well as using defects and probes with complex shapes. However, the effort of creating such models can be considerable. The models may also require many degrees of freedom resulting in expensive computations. There is also possibilities to implement complex material properties in 3D finite element models. This may include non-linear, anisotropic and inhomogeneous permeability or anisotropic and inhomogeneous conductivity. Permeability has in this work always been considered constant and homogeneous but crack descriptions has been studied by using anisotropic material conductivity (**Paper B**). There is also a possibility to study noise models by implementation of inhomogeneous or even anisotropic conductivity in the bulk material.

Figures 3.4–3.19 present FEM computations of eddy current responses due to various flaws. The input configuration used and a short interpretation of the probe-flaw interactions are included in table 3.1. The results are intended both to be used by eddy current practitioners, and to show typical configurations that might be studied using numerical modelling of EC NDE. The examples are considering paramagnetic material with $\mu_r = 1$. The width of the defect is in all computations approximately 7.5% of the penetration depth δ . The defect sizes and positions are related to the penetration depth δ in order to

achieve a more general computation scheme. The probe geometry is an absolute air-cored coil in all examples. The probe used induces circular (or eddy) currents with a diameter close to 2δ at the maximum current density on the surface, see figure 3.2.

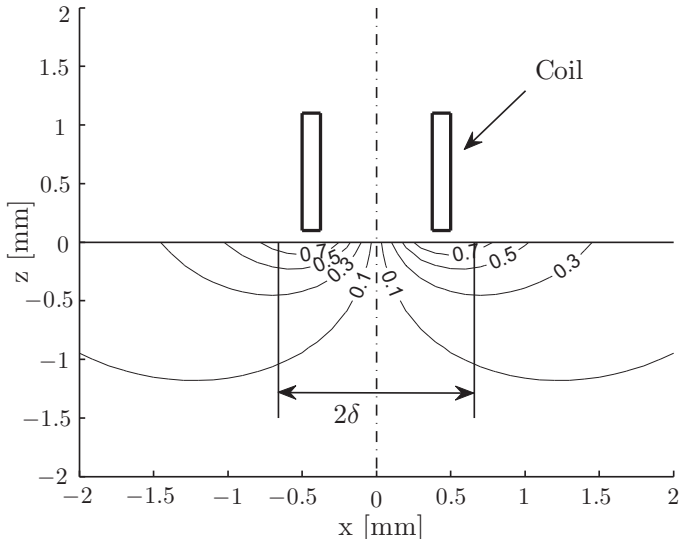


Figure 3.2: *Contour curves of induced current density as a fraction of the maximum value J_0 on the surface.*

The amplitudes in figures 3.4–3.19 are scaled with the maximum amplitude of the 2δ long, penny-shaped defect. Choosing another probe will alter the distribution of induced currents and therefore change the defect responses. The figures are, however, intended to qualitatively present the impedance response to various flaws. A view of the probe and block with mesh from one of the calculations is presented in figure 3.3. Here, the conductivity of Ti-6Al-4V is used and a frequency of 1 MHz of the applied magnetic field. Using an identical probe on a material with another conductivity will yield the same relative change in signal responses if the penetration depth is identical. The same penetration depth is achieved by changing the test frequency according to equation (2.2) on page 7.

A practical eddy current inspection includes a specific probe optimized for the procedure. The noise in the system is not captured in the computations and must therefore be considered in order to understand the detection possibilities of the real system. As an example of this, data from **Paper C** may be used as the experimental conditions are similar to the ones presented in figures 3.4–3.19. The defects here are, however, modelled as air filled and are therefore producing larger signal responses compared to closed fatigue cracks. Closed fatigue cracks may have bridging electric contacts between the faces which is shown to be present in Ti-6Al-4V (**Paper B, C**).

Table 3.1: Summary of figures

Figure	Defect type	Variable	Comments
3.4–3.6	Long, strip-like crack	Depth & tilt & sub-surface	Maximum amplitude as probe is positioned over crack centre. Phase of the impedance in X - Y plot is moving clockwise as the defect is positioned deeper into the material. It is clear that a small tilt angle has a quite limited effect on the impedance. It is also shown that the amplitude is decreasing fast with the distance as the defect is positioned sub-surface.
3.7–3.9	Spherical defect	Size & sub-surface position	Maximum amplitude appears as the probe is positioned at the side of the defect. That location is most effectively changing the induced currents. The signal drops as the probe is located over the centre of the defect as the induced currents flow around the defect. The two amplitude peaks are related to the induced current density distribution and thus the probe size. The peaks are thus positioned approximately at the same places for all defect sizes.
3.10–3.11	Rectangular defect	Length & depth	Maximum amplitude is at the corner of the defect. As the defect gets long compared to the induced current distribution there is a transition towards a single peak in amplitude as the probe is positioned over the centre. The increase in depth is causing a decrease in amplitude and a phase shift in the impedance plane.
3.12–3.13	Half-penny shaped defect	Size & tilt	The shape is similar to fatigue cracks and the signal response can be compared to rectangular defects in previous figures.
3.14–3.15	Half-penny shaped defect	Lift-off & tilt of probe	It is clear that lift-off and tilt angle of the probe is important variables that must be controlled in any EC inspection. The signal can be used to ensure alignment of the probe in a calibration procedure as a small tilt angle is breaking the symmetry of the amplitude.
3.16–3.18	Rectangular & half-penny shaped back wall defect	Size & geometry	The rectangular and half-penny shaped defect can be compared between the figures. All bulk materials are thin and the defect is positioned on the opposite side of the probe.
3.19	Edge defect	Size	Maximum amplitude appears as the probe is positioned over the centre of the defect. The inspection procedure must ensure that the positioned relative the edge is as constant as possible as there will be a significant signal change when the probe is moved over the material edge.

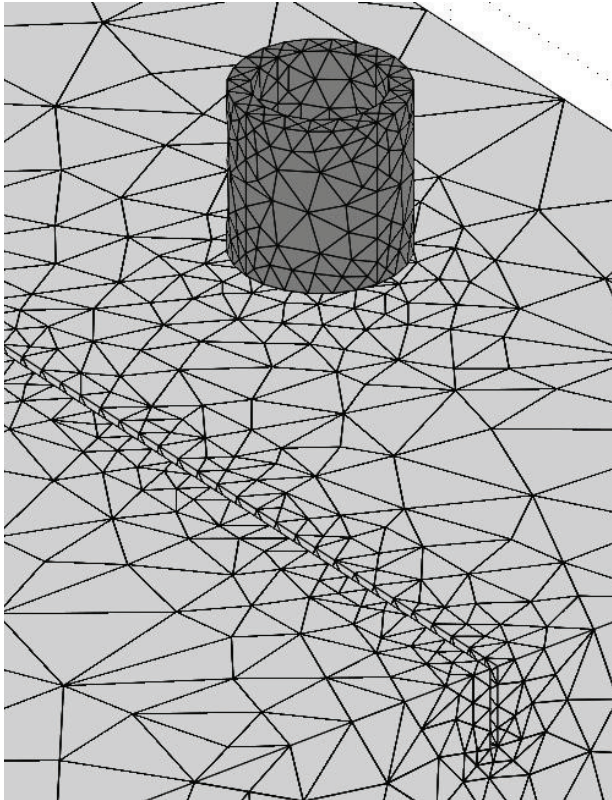
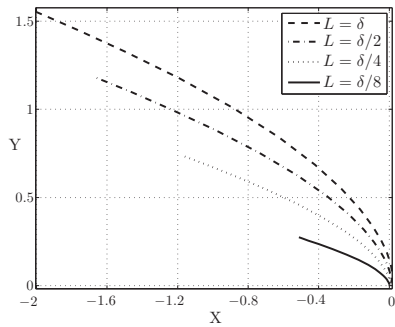
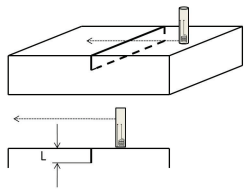
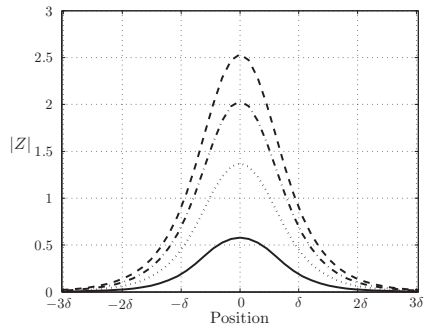


Figure 3.3: *Mesh of the probe and block in the calculation of the response from a long strip-like crack.*

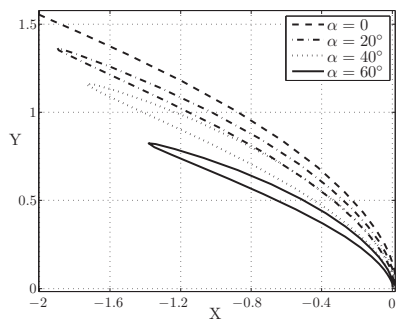
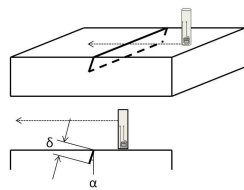


(a) Impedance plane.

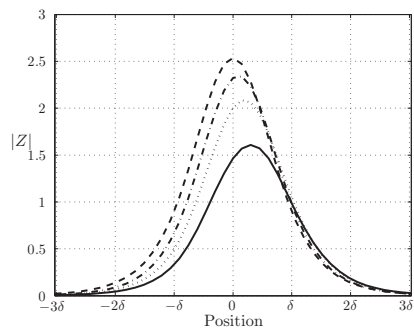


(b) Amplitude versus probe position.

Figure 3.4: Long strip-like crack with varying depth.

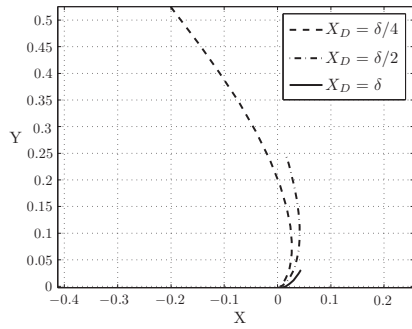
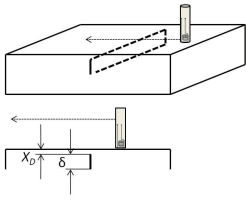


(a) Impedance plane.

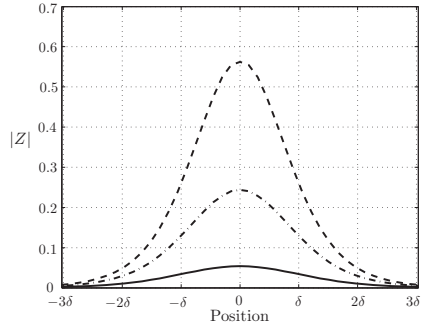


(b) Amplitude versus probe position.

Figure 3.5: Long strip-like crack with varying tilt angle.

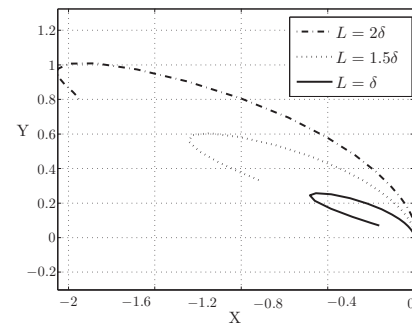
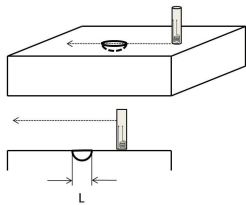


(a) Impedance plane.

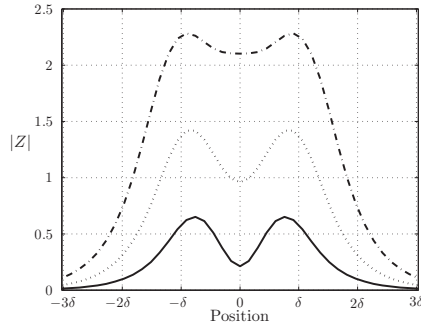


(b) Amplitude versus probe position.

Figure 3.6: Long strip-like crack, subsurface.

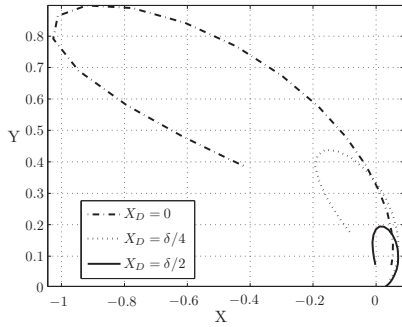
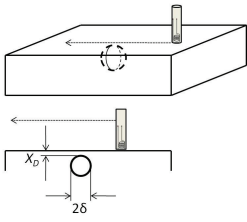


(a) Impedance plane.

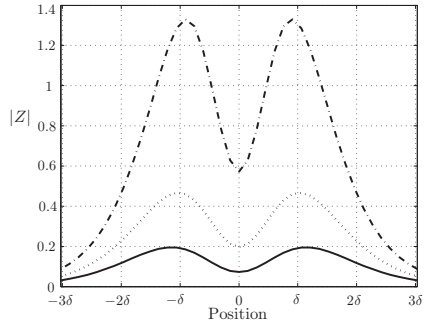


(b) Amplitude versus probe position.

Figure 3.7: Half-spherical surface defect with varying radius.

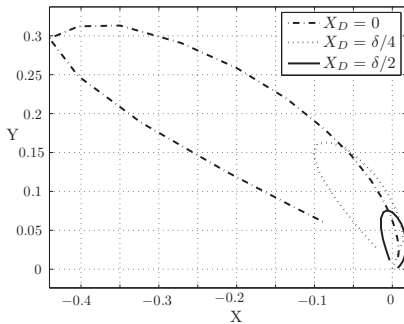
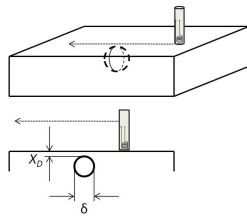


(a) Impedance plane.

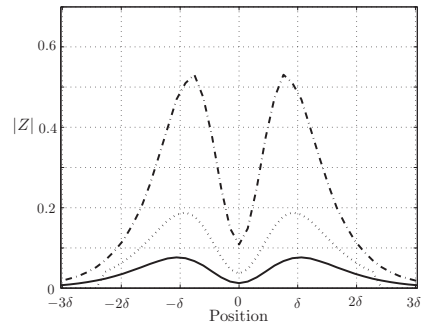


(b) Amplitude versus probe position.

Figure 3.8: Spherical subsurface defect at varying depth.

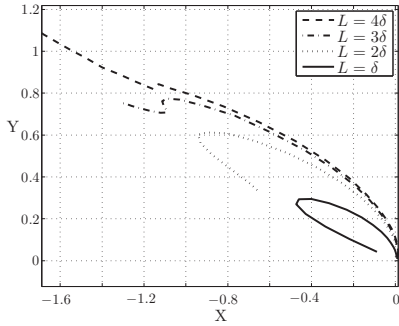
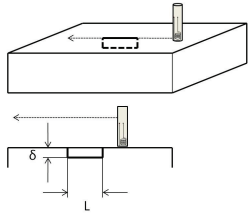


(a) Impedance plane.

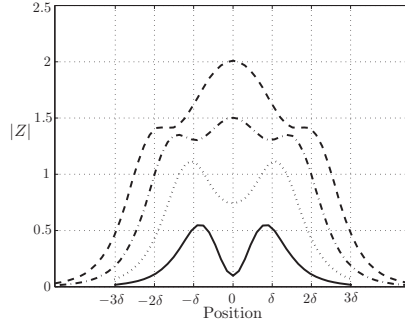


(b) Amplitude versus probe position.

Figure 3.9: Spherical subsurface defect at varying depth.

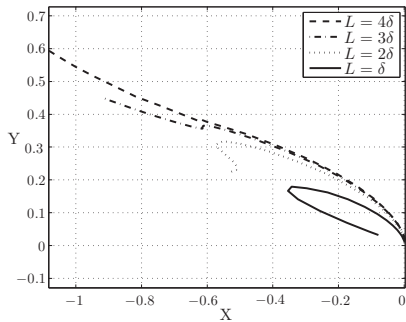
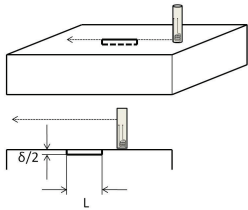


(a) Impedance plane.

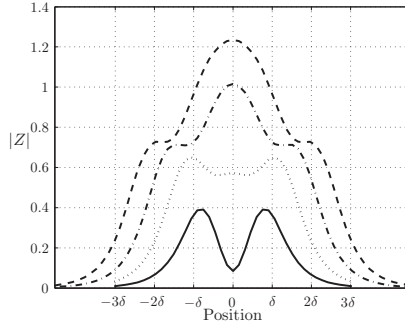


(b) Amplitude versus probe position.

Figure 3.10: Rectangular defect with constant depth and varying length.

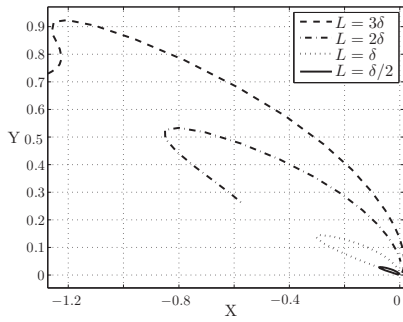
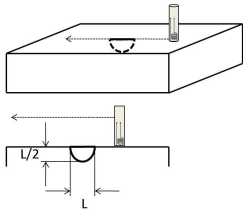


(a) Impedance plane.

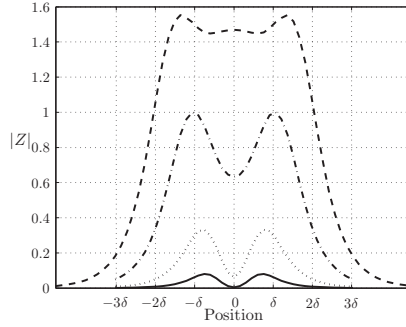


(b) Amplitude versus probe position.

Figure 3.11: Rectangular defect with constant depth and varying length.

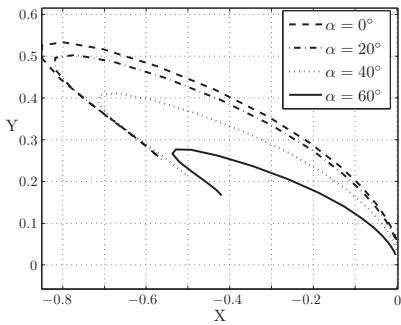
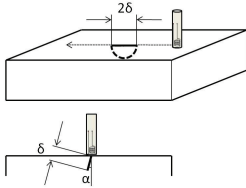


(a) Impedance plane.

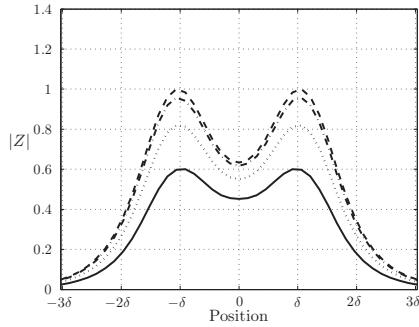


(b) Amplitude versus probe position.

Figure 3.12: Half-penny shaped defect with varying radius.

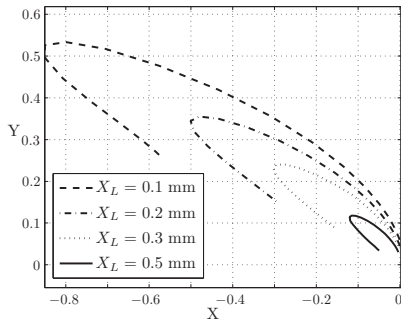
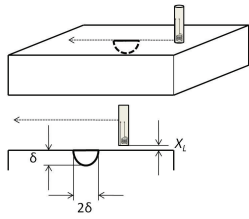


(a) Impedance plane.

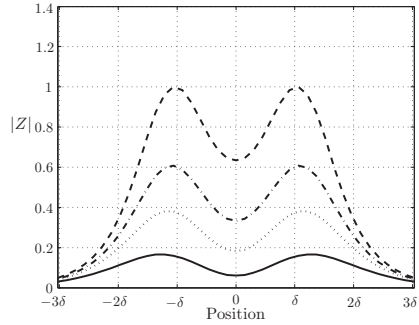


(b) Amplitude versus probe position.

Figure 3.13: Half-penny shaped defect with varying tilt angle.

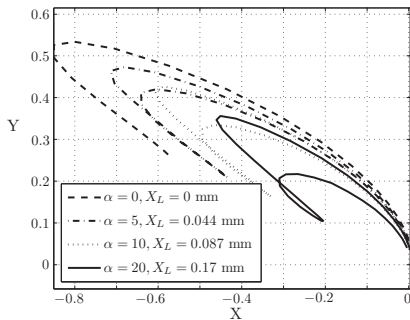
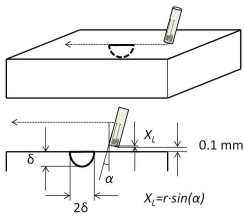


(a) Impedance plane.

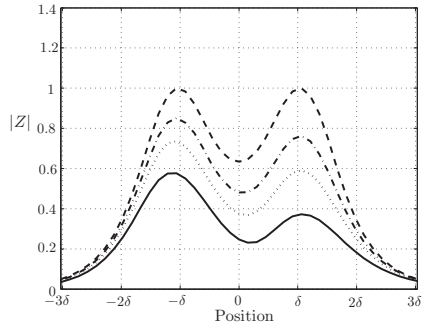


(b) Amplitude versus probe position.

Figure 3.14: Lift-off change over half-penny shaped defect.

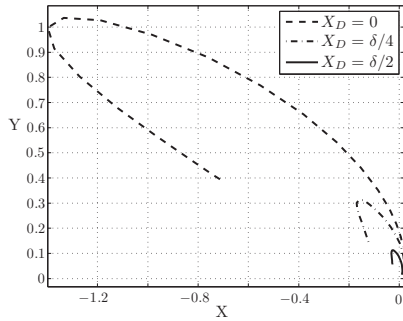
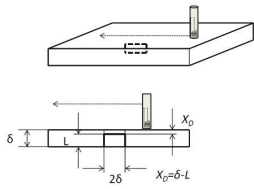


(a) Impedance plane.

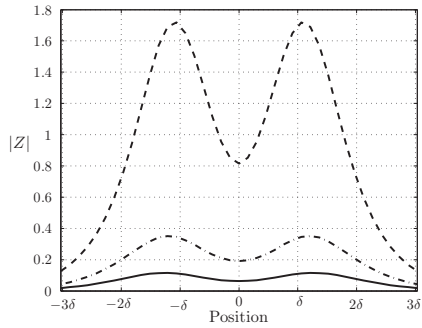


(b) Amplitude versus probe position.

Figure 3.15: Probe tilt change over half-penny shaped defect.

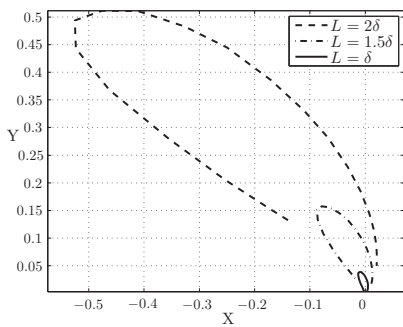
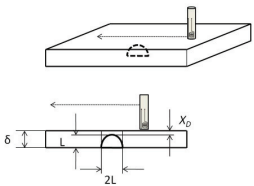


(a) Impedance plane.

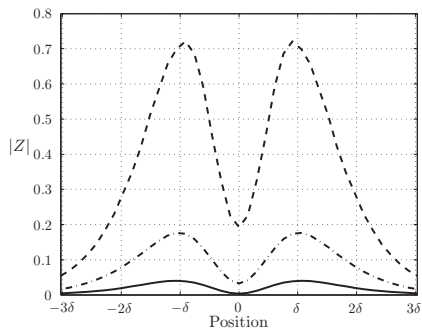


(b) Amplitude versus probe position.

Figure 3.16: Subsurface rectangular defect in thin material.

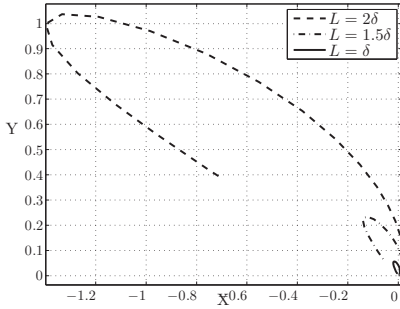
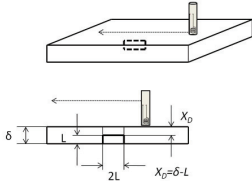


(a) Impedance plane.

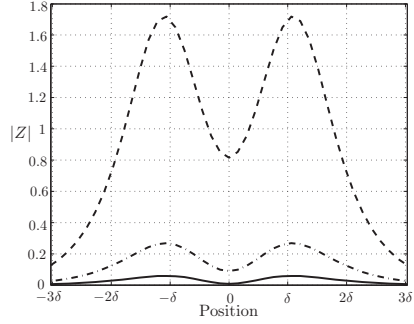


(b) Amplitude versus probe position.

Figure 3.17: Subsurface half-penny shaped defect in thin material.

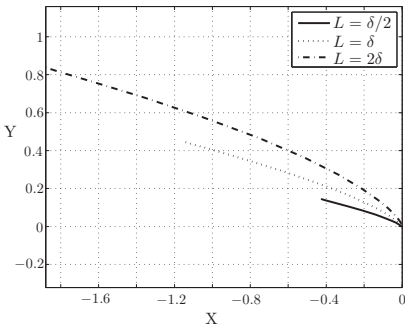
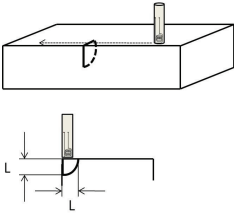


(a) Impedance plane.

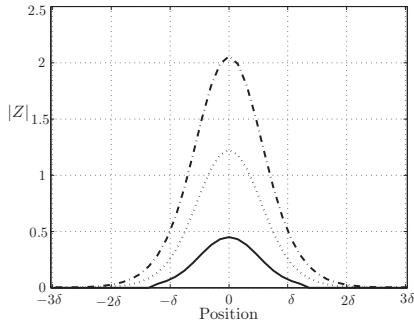


(b) Amplitude versus probe position.

Figure 3.18: Rectangular defect subsurface in thin material.



(a) Impedance plane.



(b) Amplitude versus probe position.

Figure 3.19: Edge defect.

4 Probability of detection

4.1 Introduction

One of the main goals with the work presented here is to use mathematical models in the framework of probability of detection assessments in eddy current NDE. The background of POD is presented in this chapter in order to describe this in relation to eddy current modelling. The purpose here is also to present some of the statistical background as it is most important to bare this in mind when discussing matters regarding the capability of NDE methods. Eddy current inspections are often automated with the output as a signal response proportional to a defect size parameter. It is these procedures that are addressed within this work, as the physical model in its present state does not handle the human influence. One may argue that the POD of an automated system refers to the signal presentation on the screen of the eddy current instrument and not on the actual result in the inspection protocol. This must be considered at least if there is a human involved as interpreter in the process. The limitation is assumed here and EC output data refer to the recorded signal on the screen. The data from these systems provide so-called \hat{a} versus a data (signal versus defect size) and the statistical properties must be treated accordingly. The other option is that the system gives binary data i.e. of hit or miss nature. This is common for different NDE systems such as FPI, the statistical background is presented in for example in (MIL-HDBK-1823 2009; Berens 1989) and is not discussed here.

4.2 Background

Many NDE systems are driven by the goal to detect smaller and smaller defects. When applied under these extreme conditions, not all flaws of the same size will be detected. Variations of the signal response to different defects of the same size demonstrate that POD is needed for the description of method capability. The resulting POD is depending on several factors and not only defect size. Defect size could relate for example to crack length, depth or some other characteristic parameter combination. For a given NDE application there is no possibility to know the true POD as this is a statistical property and an infinite number of samples thus are needed. The capability of the NDE system can only be demonstrated with representative experiments from which the true POD curve is estimated. The estimation technique can be based on a parametric or non-parametric approach. The parametric approach uses the information in a statistical model that is assuming some basic properties of the capability, for example that the POD increase with increasing defect size. The non-parametric approach estimates the POD at individual defect sizes, not assuming any POD model. The theoretically true POD can thus only be retrieved from a non-parametric approach not making any assumptions on the data. The result from a POD assessment results in a curve that states the probability of detecting a defect of size a . The parametric approach is the most commonly applied and is often presented together with confidence bounds due to the statistical nature of the POD model.

An experimental POD curve estimation should be conducted with the relevant procedure on representative objects with known defect sizes. The estimated POD will be subjected to statistical variation that results from all uncontrolled factors related to the inspection process. The POD result is used in the design of components when principles of damage tolerance design are applied. A commonly used design criterion within the aerospace community is that the system should manage a 90 % detection level at the criterion for damage tolerance design. The size of the defect that is the outcome from a POD assessment should be taken at the 95% lower confidence bound at this detection level. The notation for this is $a_{90/95}$.

Demonstration of a NDE process can be made by means of a subset of a full POD. Based on statistical sampling theory, 29 successes in 29 trials at one flaw size give a 95% confidence that this flaw size will be found 90 % of the time. Different conditions apply for other levels of confidence (Yee et al. 1976). This method provides less information about the inspection system than using a range of flaw sizes for test specimens. It is used mainly as a demonstration if the capability is known a priori. This point estimation method is useful for qualifying personnel or procedure when the general capabilities of the process are known (MIL-HDBK-1823 2009). It is however important to also demonstrate that the POD curve is increasing with increasing defect size, which is vital for a valid result, but not always true.

Other methods to quantify POD other than the 29/29 point estimate method, consider the ratio between the number, n , of cracks detected, divided by the total number, N , of cracks inspected. This is assumed to be a reasonable assessment of system inspection capability with $POD = n/N$. The result from such an assessment is a single number for the entire range of crack sizes. However, since larger cracks in general are easier to find than smaller ones, cracks are often grouped according to size (Yee et al. 1976; Rummel 1982). Grouping specimens this way improve the resolution in crack size. However, the resolution in POD and associated confidence levels suffer because of fewer specimens in each range. This concept has been further utilized to treat the validity of POD data (Generazio 2009). A variation of grouping methods were demonstrated and it was argued that they all suffered from problems with the calculation of the lower confidence bound (Berens and Hovey 1981). The data traditionally used in these assessments were of hit/miss nature. Another use of the binary (hit/miss) output was to assume a mathematical relationship between POD and size i.e. a parametric POD model, and then estimate the parameters of this model with the use of a statistical framework. The amplitude, \hat{a} , of the output signal has made it possible to extract more information and improve the $POD(a)$ estimates. The methods presented in (Generazio 2009) may be applied for such data by conversion of the signal response to binary output. There are thus two main approaches to estimate the POD. In this work the methods of Berens are mainly used (Berens 1989). This method represents the most widely used technique in aerospace applications with a well described guideline (MIL-HDBK-1823 2009) also thoroughly described in (Gandossi and Annis 2010; Annis and Vukelich 1993).

4.3 Considerations for EC POD

An understanding of the sources of variations and relevant parameters in an eddy current procedure are critical in order to build a POD curve for a method procedure. A large number of parameters can be related to variations in a procedure and it is important to conclude the important ones with an impact on the method capability. For a given procedure there are usually a set of variables that may be considered as fixed, stated in the procedure specification. These variables are important concerning the value but are not representing a significant influence to variations in the flaw response. Table 4.1 presents the typical parameters belonging to an eddy current procedure, divided in influencing and those usually considered fixed. The influencing parameters are important to consider both regarding their nominal values but also their distributions. Variations due to properties of a surface connected crack are also included in the table. The POD curve is built under the assumption that defects of equal sizes give different responses and all variables that may have an impact on this must be evaluated. The table shows the variables that must be considered here, but others may apply for specific procedures, see for example (ENIQ 2005). The characteristics of the variables can be broken down to a number of individual properties which may not be relevant for an experimental procedure but are important for a model based POD assessment.

Table 4.1: Parameters related to the capability of eddy current procedures

Procedure variations	Crack variations	Fixed
Inspector changes/conditions	Size	Test frequency
Sensor changes	Shape	Probe design
Sensor positioning	Crack location	Scan plan
Loading of component	Orientation	Scanning index/speed
Position of component	Tilt	HP/LP filters
Calibration	Width	Threshold levels
Calibration object (if varied)	Electric contact	Hardware
Repetition	Oxides/Chemistry	Signal capture/digitalisation

4.4 Parametric \hat{a} versus a methodology

Eddy current data sampled from an automated or semi-automated system respond to the individual defect with a specific impedance value. The impedance response is depending on several factors coupled to the defect as well as the surrounding material and status of the inspection process. The signal response can easily be recorded and allow the evaluation of every defect of size a to be related to a signal response \hat{a} . The output \hat{a} represents some kind of impedance signal measure, often referred to a specific calibration value. The \hat{a} versus a methodology, which nearly always is considered for eddy current NDE, has a few characteristic parameters that must be considered when building the parametric POD curve. One of the most significant is the noise threshold \hat{a}_{th} which gives a level where it is not possible to distinguish between noise and signal. Figure 2.4 gives

an example of two different noise levels. Another important parameter is the decision threshold \hat{a}_{dec} which may in practice be selected as the last step when creating the POD curve. A decision threshold too close to the noise level will cause an increased probability of false alarms (PFA). A signal due to a flaw that is indistinguishable from the system noise is said to be left censored. The right censoring value corresponds to the maximum possible signal at the level of \hat{a}_{sat} , which may occur in eddy current procedures as the signal saturates in the selected volt range on the screen.

If $g_a(\hat{a})$ represents the probability density function for the system output parameter \hat{a} at the specific flaw size a , the $POD(a)$ is defined as

$$POD(a) = \int_{\hat{a}_{dec}}^{\infty} g_a(\hat{a}) d\hat{a} \quad (4.1)$$

The $POD(a)$ function can thus be obtained from the relation between a and \hat{a} . The standard approach to establish the function $g_a(\hat{a})$ assumes that the correlating function defines the mean of $g_a(\hat{a})$ and that the random error term is constant $\hat{a} = \mu(a) + \epsilon$ (Berens 1989). The random characteristics of ϵ defines the probability density of $g_a(\hat{a})$ around the mean $\mu(a)$ and should be normally distributed with constant variance for all defect sizes in the used parametric POD model. The next step is to find a proper function to describe the relation between \hat{a} and a . It is common to describe NDE data using $\log(a)$ and $\log(\hat{a})$. It is, however, pointed out in (MIL-HDBK-1823 2009) that linear relations between $\log(a)$ and \hat{a} , a and $\log(\hat{a})$ as well as a and \hat{a} should also be considered. The choice should be that which appears to describe the data best by a straight line and a constant variance of the data. Statistical tests can be used for guidance. In figure 4.1 we have an example of a result from an eddy current inspection. We ignore the procedure and concentrate on the statistical treatment of the data in order to generate the POD curve. The residuals are plotted in figure 4.2 and it can be argued that the \hat{a} versus a data qualifies best for the parametric POD model. The \hat{a} versus $\log(a)$ and $\log(\hat{a})$ versus a show that higher order terms should be added to the linear model. The $\log(\hat{a})$ versus $\log(a)$ represents a situation where the variance of the observations is decreasing with larger values of $\log(a)$. Using the \hat{a} versus a relation give

$$\hat{a} = \beta_0 + \beta_1 a + \epsilon \quad (4.2)$$

where ϵ is normally distributed with zero mean and a constant standard deviation σ_ϵ . Under these assumptions, we arrive at a parametric POD. The $POD(a)$ function is calculated by $POD(a) = \text{Probability}[\hat{a} > \hat{a}_{dec}]$ which gives

$$POD(a) = \Phi \left[\frac{a - (\hat{a}_{dec} - \beta_0)/\beta_1}{\sigma_\epsilon/\beta_1} \right] \quad (4.3)$$

where Φ is the cumulative normal distribution function with mean and standard deviation according to

$$\mu = \frac{\hat{a}_{dec} - \beta_0}{\beta_1} \quad (4.4)$$

$$\sigma = \frac{\sigma_\epsilon}{\beta_1} \quad (4.5)$$

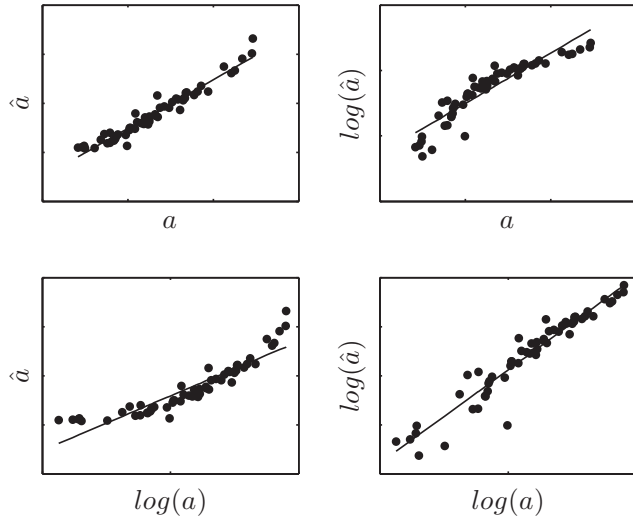


Figure 4.1: *Regressions of test data.*

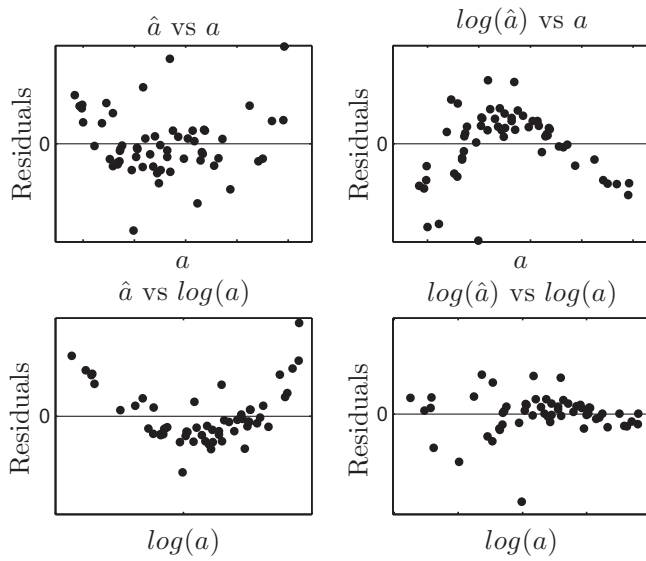


Figure 4.2: *Residuals*

Parameter estimation can be based on the principles of maximum likelihood. Likelihood is similar to probability but describes the behaviour of the parameters given the data. This provides the model parameters and estimates their variability which is used to create the $POD(a)$ function and its confidence bound. Let (X_i, Y_i) represent the outcome of the i :th inspection (a_i, \hat{a}_i) and let $f(X_i, \boldsymbol{\theta})$ be the probability of obtaining X_i . The vector $\boldsymbol{\theta}$ holds all model parameters, which in this case are represented by $\boldsymbol{\theta} = (\beta_0, \beta_1, \sigma_\epsilon)$. Hence, $f(X_i, \boldsymbol{\theta})$ is a normal density function given by $\mathcal{N}(\beta_0 + \beta_1 a, \sigma_\epsilon)$. The likelihood L is given by the function

$$L(\boldsymbol{\theta}) = \prod_i f(X_i, \boldsymbol{\theta}) \quad (4.6)$$

The maximum likelihood is the value $\hat{\boldsymbol{\theta}}$ that maximizes $L(\boldsymbol{\theta})$ for a given outcome X_i . For some models it is more convenient to work with $\log(L(\boldsymbol{\theta}))$ which is also maximized at $\hat{\boldsymbol{\theta}}$. The maximum likelihood estimates for the model parameters are therefore given by the solution to the equations

$$\frac{\partial \log(L(\boldsymbol{\theta}))}{\partial \theta_k} = 0 \quad (4.7)$$

The \hat{a} values that falls below the noise threshold or above the saturation limit must be treated properly when estimating the model parameters β_0 , β_1 and σ_ϵ . The probability of obtaining a value \hat{a}_i below the noise threshold for the i th flaw is $\Phi(\hat{a}_{th})$ and above the saturation limit is $1 - \Phi(\hat{a}_{sat})$. The log-likelihood for a number of independent observations is

$$\begin{aligned} \log L(\beta_0, \beta_1, \sigma_\epsilon) &= -\frac{n}{2} \log(2\pi) - n \log(\sigma_\epsilon) - \frac{1}{2\sigma_\epsilon^2} \sum_i^n [Y_i - (\beta_0 + \beta_1 X_i)]^2 \\ &\quad + \sum_{i_{th}} \log(\Phi_{i_{th}}(y_{th})) + \sum_{i_{sat}} \log(1 - \Phi_{i_{sat}}(y_{sat})) \end{aligned} \quad (4.8)$$

where n is the number of uncensored values, i_{th} and i_{sat} are the left and right censored observations, respectively. The maximum likelihood estimates are asymptotically unbiased, however, in this case when there are no censored values it is possible to use the least square estimate $\hat{\sigma}_\epsilon^2 = \sum_i e_i / (n - 2)$. This gives the expected value $E[\hat{\sigma}_\epsilon^2] = \sigma_\epsilon^2$ in contrast of the asymptotically unbiased maximum likelihood estimator $E[\hat{\sigma}_{\epsilon, ML}^2] = \sigma_\epsilon^2 - \sigma_\epsilon^2/n$. With this data it is possible to determine the confidence interval on the regression of the data as well as determine the $POD(a)$ function as presented in figure 4.3. Lines are also introduced which indicates the 90% prediction interval for a new observation. It is clear from the figure this treatment does not require all crack sizes to be represented in the range where the POD curve is rapidly changing. The parametric model is using information from all cracks to estimate the variability and mean values at each size which gives the POD curve.

The $POD(a)$ function is created as a cumulative normal distribution function with estimated parameters from (4.4) and (4.5) based on the maximum likelihood analysis. The next step is to create the lower 95% confidence limit which by convention often is used as the defect size design value based on a POD assessment. The uncertainty of the

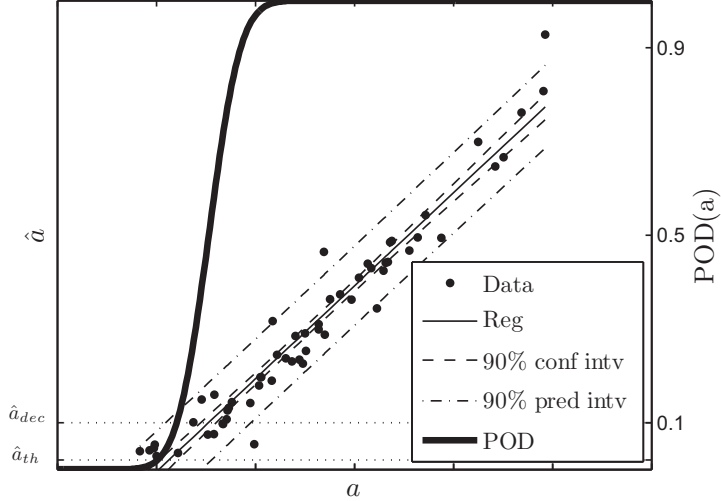


Figure 4.3: *POD model adapted to data.*

POD curve parameters is associated with the estimation of the regression parameters $(\hat{\beta}_0, \hat{\beta}_1, \hat{\sigma}_\epsilon)$. The estimated POD curve parameters $(\hat{\mu}, \hat{\sigma})$ vary around the true values (μ, σ) . The confidence band can be constructed by the principles of (Cheng and Iles 1983; Cheng and Iles 1988) or by the Wald method as presented in (MIL-HDBK-1823 2009), the latter is used in **Paper C**. The lower 95% confidence bound can now be added to the *POD* curve which gives the $a_{90/95}$ value according to figure 4.4.

The *POD* curve and the lower confidence limit give an estimation of the detection capability of the procedure and what defects could be missed by the NDE system. It couples directly to the procedure, defect, hardware and the human influence. When demonstrating eddy current procedures it is important to show that the result holds for all equipment intended for use, particularly probes. It is also important to show that parameters such as lift-off are within the prescribed limits of the procedure. The steps presented here show how the typical parametric *POD* curve is retrieved. This model must be used carefully and the input data must follow the required statistical properties, independent data, constant variance and normally distributed residuals², as given by (Berens and Hovey 1981; Berens 1989).

²The model requires also linearity in regression parameters, which is omitted in the discussion here.

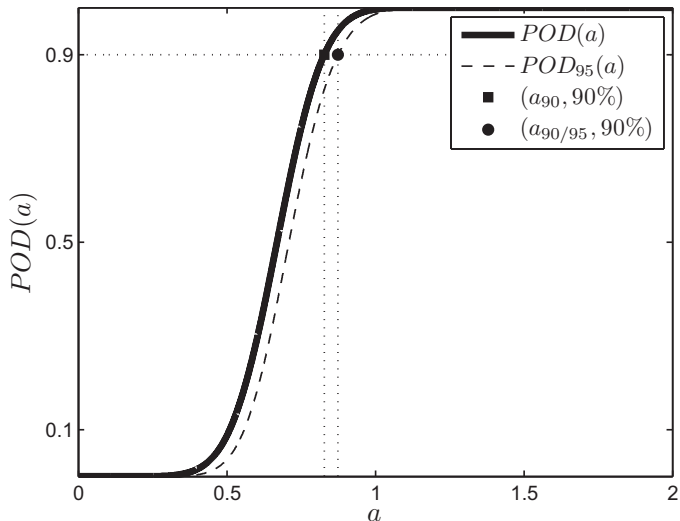


Figure 4.4: *POD curve and the lower 95% confidence limit.*

4.5 Model based POD

To determine a POD curve involves the creation of relevant test objects in sufficiently large numbers and with defects of various sizes. Such objects are in general expensive and it is a time consuming process to establish them. If the inspection procedure is applied to another material or in geometries different from that of the test objects, the POD most likely is no longer valid. It is common in eddy current testing to use flat test objects with fatigue cracks. These test objects may be argued to be valid even if the procedure is applied on curved surfaces. One of the problems is the cost involved with creating real fatigue cracks in component mock-ups. This difficulty is sometimes handled with the delta POD approach. In that case artificial defects that are simple to manufacture, for example EDM notches, are produced in complex geometries. These defects are used for the POD assessment by comparing the procedure in a simple geometry on real and artificial defects. This gives the possibility to transfer the information to the POD on the more complex part with real defects. This methodology is sometimes also called the transfer function approach (Thompson 2001; Thompson 2007).

Model based POD has the potential to effectively evaluate process changes and estimate results in complex geometries. It can also aid in the POD assessment using transfer functions. The nature of the models determines to some extent how the result can be employed. In order to produce results as input to design of components, the models need to be validated and include defects with characteristics close to real defects. The variability of all other relevant parameters must be included in the model. It is also

important to generate an estimation of the POD that is conservative in its nature. These points represent the ultimate goal. Models today may however give input to procedure set up, generate fast results in an early stage and estimate effects of variations in geometry, material, equipment, procedure and flaws. The approach for model based POD used on eddy current procedures has been studied prior to this work but not with the whole complexity of the real procedure included (Beissner and Graves III 1990; Nakagawa and Beissner 1990; Nakagawa et al. 1990; Rajesh et al. 1993). General discussions on the topic are quite rare but at least the articles (Wall 1997; Thompson 2007) and the chapter on the topic in (MIL-HDBK-1823 2009) are well worth reading.

There are two main approaches that should be mentioned concerning model based POD, see figure 4.5. The first approach is the delta POD concept using transfer functions. By the use of transfer functions the real POD is estimated based on the difference between artificial and real defects in a simple geometry, using for example plane surface test pieces. The base line POD estimated in a simple geometry gives the estimated \hat{a} versus a parameters ($\hat{\xi}_0, \hat{\xi}_1, \hat{\sigma}_\epsilon$). The knowledge deduced by the transfer function approach will then allow the computation of a new set of parameters ($\hat{\beta}_0, \hat{\beta}_1, \hat{\sigma}_\epsilon$), which are used for estimation of the POD in the complex geometry. A simulation based approach may substitute the experimental trials on complex geometries but still using simple defects. It can also be the case that some parameters of variation are studied in a model and some in experimental procedures, for example capturing the influence from humans. There is also a possibility to use measured noise characteristics on the nominal model based response (Knopp et al. 2007). However, this approach does not include variations in defects characteristics.

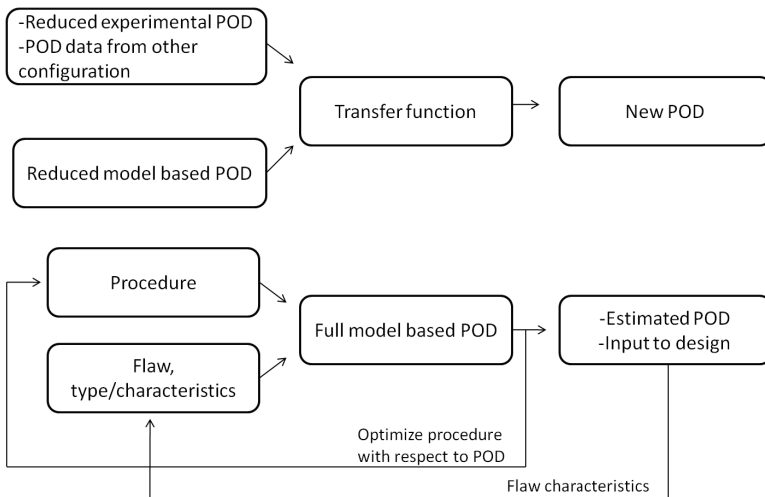


Figure 4.5: *The use of model based POD.*

The second approach is to generate a full model based POD. This methodology can in turn be divided into two different concepts based on the access and treatment of modelled data. The idea is to systematically identify the factors that influence the variability of the NDE procedure. Noise and signal factors must then be included in the model. If computations are expensive such an approach can be used to retrieve synthetic data and treat this in analogue to experimentally obtained data (Dominguez and Jenson 2010) and also (**Paper C**). This concept results in a parametric POD using the statistical model described in section 4.4. The other approach for a full model based POD is to estimate the signal distribution for a defect of a specific size, see figure 4.6. The signal distributions are depending on the variation of procedure parameters and defect characteristics. Noise may also be estimated in order to estimate the probability of false alarms (PFA). Such an approach requires a Monte Carlo method where a large number of parameter configurations are used at each defect size. This concept is based on a large number of computations, which thus must be efficient. The result is not influenced by any statistical model and is thus representing a non-parametric POD. This approach can therefore also be used to gain deeper understanding of the concept and statistical tools used for POD estimation.

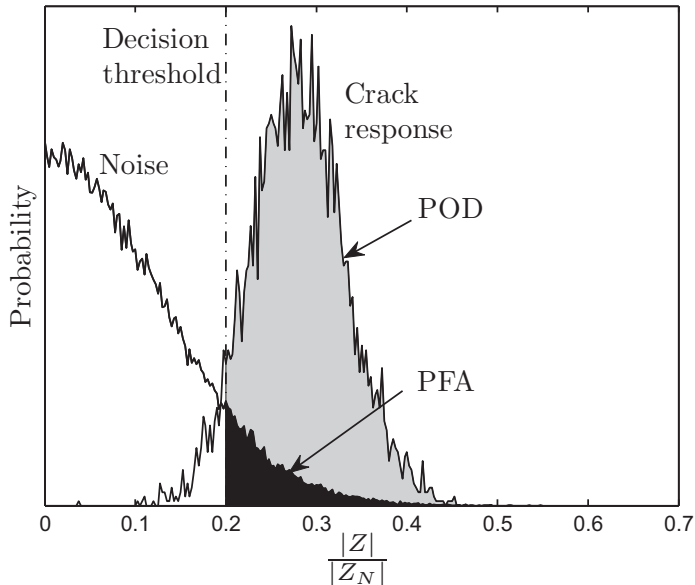


Figure 4.6: *Distributions of noise and signal from a crack retrieved in a modelled eddy current procedure.*

5 Summaries of appended papers

Paper A: *Modelling a Differential Sensor in Eddy Current Non-Destructive Evaluation*

A 3D validation case from the literature is studied. Using this framework, the set up of a FE model is developed with the goal to arrive at an applicable methodology for EC modelling. The FE model with the probe impedance as output variable must produce results with good precision. Model based POD requires small signal variations to be captured. Axisymmetric FE models and also analytic models are successfully used here to gain understanding of how to build efficient 3D FE models. Conclusions about errors introduced from truncation of the outer boundary and mesh configurations are drawn.

Paper B: *Finite Element Modelling of Closed Cracks in Eddy Current Testing*

The closed fatigue crack in Ti-6AL-4V is studied. An experimental set up for evaluation of the establishment of electric connections between the crack faces is developed. Different kinds of contact models are tested and the importance and complexity of the contact within closed fatigue cracks are showed. It is concluded that this requires a complex model with several parameters. It is however possible to resemble the contact characteristics in a model. This is important in order to describe the natural defect and to include its properties in a model based POD assessment. The experimental work presented shows the impact from the characteristics of the crack to the eddy current response as surface oxides build up on the crack faces. The importance of describing the electric contacts within cracks in Ti-6AL-4V is enlightened.

Paper C: *Comparison of Experimental and Model Based POD in a Simplified Eddy Current Procedure*

A realistic procedure including relevant defects is evaluated in both experiments and in a numerical model. This work serves as a first validation of the model based POD approach and is regarding the usage of synthetic data treated analogously with experimental data. It is shown that it is possible to get good agreement, but this requires the development of a satisfying fatigue crack model. The crack model describes the characteristics in a statistical approach, not focusing on individual defects. The model is constructed based on a limited number of experiments. Electric contacts between the crack surfaces are needed to explain the signal response characteristics of the closed fatigue cracks used in the experimental POD assessment. The results show good agreement in estimation of POD based on numerical and experimental data, respectively.

6 Conclusions and future work

The goal of this work has been to develop a FE model that is able to predict EC signal responses in realistic NDE configurations. The model is developed to include distribution of several parameters coupled to a typical procedure. The computations must be efficient in order to estimate the method capability in the framework of POD. The initial part of the work has focused on the modelling aspects and the description of the fatigue crack. The second part has focused on how to implement procedure variations and to build a methodology for model based POD. The work has continuously been accompanied with experimental validations. The points below summarize the major conclusions from **Papers A-C**.

- The outer boundaries in a FE model of eddy current are describing the fields at a position placed infinitely far away from the probe and flaw interaction. The truncation can be made at the position where the magnetic vector potential has decreased to 1% of its maximum amplitude. This position can efficiently be evaluated in a simplified model.
- The predication of EC impedance signals from an absolute coil as well as a receiving coil can be predicted by the numerical model.
- Electrical contacts within a closed fatigue crack can be evaluated in an experimental set up using eddy current measurements as different levels of static loads are applied across the crack.
- Electrical contacts between crack faces are important to include in a model of a closed fatigue crack in Ti-6AL-4V in order to get realistic signal predictions. The small width of a fatigue crack is also important to include in a model even if the electric contacts are non-significant within the crack.
- The variations of parameters in an eddy current procedure can be captured in a FE model. This enable the usage of model based POD for realistic procedures.

Modelling of the natural, real, defect is a challenging quest. Regarding POD this objective is reduced to capture the statistical behaviour of defects. Even in that sense it is important to present a description that represents the defects at all possible inspection configurations. This development starts with a methodology to evaluate the electrical contacts between the crack faces more thoroughly by for example considering many inspection frequencies. This will give the possibility to describe and characterize individual defects or a specific set used for POD. It is also important to include different materials in the evaluation. Modelling the natural defect can also show how special features influence the detection possibilities. This goal does not only include a description of the electrical contacts within a defect but also its 3D geometry. There are also important steps regarding the use of such defects in model based POD assessments, for example to determine the variability of the characteristic parameters of the defect. A model based non-parametric POD used for studying the signal distribution, should be compared to experimental data. Such a model can be used to study variations in procedure parameters in relation to the POD

estimation. The model based POD concept should also be applied to complex geometries. The approach could in that case also consider the use of transfer functions. Such studies will aid in the development and understanding of new eddy current inspection procedures. A physical model can be a useful tool in several steps when developing a procedure. The use of such models may in the future be a natural and vital part in the process of understanding the limitations, capability and reliability of a NDE procedure.

References

- Annis, C. and Vukelich, S. (1993). *A Recommended Methodology for Quantifying NDE/NDI Based on Aircraft Engine Experience*. AGARD lecture series 190. AGARD-LS-190. North Atlantic Treaty Organization, Advisory Group for Aerospace Research and Development.
- ASIAC (1980). *The history of the aircraft structural integrity program*. Report No. 680.1B. San Carlos, California: Aerospace structures information and analysis center (ASIAC).
- Auld, B.A. and Moulder, J.C. (1999). “Review of Advances in Quatitative Eddy Current Nondestructive Evaluation”. In: *Journal of Nondestructive Evaluation* 18.1, pp. 3–36.
- Auld, B.A., Jefferies, S.R., and Moulder, J.C. (1988). “Eddy-Current Signal Analysis and Inversion for Semielliptical Surface Cracks”. In: *Journal of Nondestructive Evaluation* 10.1/2, pp. 79–94.
- Beissner, R.E. and Graves III, J.S. (1990). “Computer Modeling of Eddy Current Probability of Crack Detection”. In: *Review of progress in quantitative nondestructive evaluation*. Ed. by D.O. Thompson and D.E. Chimenti. Vol. 9A. Plenum Press, pp. 885–891.
- Berens, A. P. (1989). “NDE reliability data analysis”. In: *Nondestructive Evaluation and Quality Control*. Vol. 17. ASM Metals Handbook. ASM International, pp. 689–701.
- Berens, A.P. and Hovey, P.W. (1981). *Evaluation of NDE Reliability Characterization*. AFWAL-TR-81-4160. Wright-Patterson Air Force Base: Air Force Wright Aeronautical Laboratories.
- Bíró, O. (1999). “Edge element formulations of eddy current problems”. In: *Comput. Methods Appl. Mech. Eng.* 169.3–4, pp. 391–405.
- Bíró, O. and Preis, K. (1989). “On the use of the magnetic vector potential in the finite element analysis of three-dimensional eddy current problems”. In: *IEEE Trans. Magn.* 25.4, pp. 3145–3159.
- Bíró, O. and Preis, K. (1990). “Finite Element Analysis of 3-D Eddy Currents”. In: *IEEE Transactions on Magnetics* 26.2, pp. 418–423.
- Blitz, J. (1997). *Electrical and magnetic methods of non-destructive testing*. 2nd ed. Non-destructive evaluation series. London: Chapman and Hall.
- Blodgett, M.P. and Nagy, P.B. (2004). “Eddy Current Assessment of Near-Surface Residual Stress in Shot-Peened Nickel-Base Superalloys”. In: *Journal of Nondestructive Evaluation* 23.3, pp. 107–123.
- Blodgett, M.P., Hassan, W., and Nagy, P.B. (2000). “Theoretical and Experimental Investigations of the Lateral Resolution of Eddy Current Imaging”. In: *Materials Evaluation* 58.5, pp. 647–654.
- Bondeson, A., Rylander, T., and Ingelström, P. (2005). *Computational Electromagnetics*. Texts in applied mathematics 51. New York: Springer.
- Bossavit, A. (1998). *Computational electromagnetism*. San Diego, CA: Academic Press Inc.
- Cecco, V.S., Van Drunen, G., and Sharp, F.L. (1983). *Eddy current manual Volym 1*. Chalk River Nuclear Laboratories.
- Cheng, R.C.H. and Iles, T.C. (1983). “Confidence Bands for Cumulative Distribution Functions of Continuous Random Variables”. In: *Technometrics* 25.1, pp. 77–86.

- Cheng, R.C.H. and Iles, T.C. (1988). "One-Sided Confidence Bands for Cumulative Distribution Functions". In: *Technometrics* 30.2, pp. 155–159.
- Dodd, C. and Deeds, W. (1968). "Analytical solutions to eddy-current probe-coil problems". In: *Journal of Applied Physics* 39.6, pp. 2829–2838.
- Dogaru, T. and Smith, S.T. (2001). "Giant Magnetoresistance-Based Eddy-Current Sensor". In: *IEEE Transactions on Magnetics* 37.5, pp. 3831–3838.
- Dominguez, N. and Jenson, F. (2010). "Simulation assisted POD of a High Frequency Eddy Current Inspection Procedure". In: *Proceedings of the 10th European Conference on Non-Destructive Testing*. European Conference on Non-Destructive Testing (Moscow).
- ENIQ (2005). *ENIQ Recommended Practice 1 Influential / Essential Parameters*. ENIQ Report nr. 24 EUR 21751 EN.
- Feng, Y., Blodgett, M.P., and Nagy, P.B. (2006). "Eddy Current Assessment of Near-Surface Residual Stress in Shot-Peened Inhomogeneous Nickel-Base Superalloys". In: *Journal of Nondestructive Evaluation* 25.1, pp. 17–28.
- Fetzer, J., Kurz, S., and Lehner, G. (1997). "The Coupling of Boundary Elements and Finite Elements for Nondestructive Testing Applications". In: *IEEE Transactions on Magnetics* 33.1, pp. 677–681.
- Förster, F. (1983). "The First Picture: A Review of the Initial Steps in the Development of Eight Branches of Nondestructive Material Testing". In: *Materials Evaluation* 41.3, pp. 1477–1488.
- Gandossi, L. and Annis, C. (2010). *ENIQ Probability of Detection Curves: Statistical Best-Practices*. ENIQ Report nr. 41 EUR 24429 EN.
- Generazio, E.R. (2009). "Design of Experiments for Validating Probability of Detection Capability of NDT Systems and for Qualification of Inspectors". In: *Materials Evaluation* 67.6, pp. 730–738.
- Goldfine, N. and al., et (2005). "Weld Characterization using Eddy Current Sensors and Arrays". In: *US Patent 20050017713A1*.
- Grimberg, R. et al. (2006). "2D Eddy current sensor array". In: *NDT & E International* 39, 264–271.
- Hagemaijer, D.J. (1990). *Fundamentals of eddy current testing*. American Society for Nondestructive Testing.
- Hughes, D.E. (1879). "Induction Balance and Experimental Researches Therewith". In: *The London, Edinburgh and Dublin Philosophical Magazine and Journal of Science Fifth Series* 8.46, pp. 50–57.
- Ida, N. (1988). "Alternative approaches to the numerical calculation of impedance". In: *NDT International* 21.1, pp. 27–35.
- Ida, N. (1995). *Numerical modeling for electromagnetic non-destructive evaluation*. Engineering NDE. London: Chapman & Hall.
- Ida, N., Palanisamy, R., and Lord, W. (1983a). "Eddy Current Probe Design Using Finite Element Analysis". In: *Materials Evaluation* 41.12, pp. 1389–1394.
- Ida, N., Betzold, K., and Lord, W. (1983b). "Finite Element Modeling of Absolute Eddy Current Probe Signals". In: *Journal of Nondestructive Evaluation* 3.3, pp. 147–154.
- Ida, N., Betzold, K., and Lord, W. (1985). "A Finite Element Model for Three-Dimensional Eddy Current NDT Phenomena". In: *IEEE Transactions on Magnetics* 21.6, pp. 2635–2643.

- Ida, N., Betzold, K., and Lord, W. (1987). "Efficient Treatment of Infinite Boundaries in Electromagnetic Field Problems". In: *COMPEL* 6.3, pp. 137–149.
- Knopp, J.S. et al. (2007). "Investigation of a Model-Assisted Approach to Probability of Detection Evaluation". In: *AIP Conf. Proc.* Review of Progress in Quantitative Nondestructive Evaluation (Portland, Oregon (USA)). Vol. 894, pp. 1775–1782.
- Larsson, L. and Rosell, A. (2011). "The transition matrix method for a 2D eddy current interaction problem". In: Review of progress in quantitative nondestructive evaluation (Burlington, Vermont). (To be published in conference proceedings).
- Liu, Y. et al. (2002). "Eddy-Current Computations Using Adaptive Grids and Edge Elements". In: *IEEE Transactions on Magnetics* 38.2, pp. 449–452.
- Marchand, B., Decitre, J.M., and Casula, O. (2010). "Flexible and Array Eddy Current Probes for Fast Inspection of Complex Parts". In: *Review of progress in quantitative nondestructive evaluation*. Ed. by D.O. Thompson and D.E. Chimenti. Vol. 29, pp. 385–392.
- McMaster, R.C. (1959). *Nondestructive Testing Handbook*. Vol. 2. New York: Ronald Press Co.
- McMaster, R.C., McIntire, P., and Mester, M.L. (1986). *Eddy current, flux leakage and microwave nondestructive testing*. 2nd ed. Vol. 4. Nondestructive testing handbook. American Society for Nondestructive Testing.
- MIL-HDBK-1823 (2009). *Nondestructive evaluation system reliability assessment*. USA Department of Defense Handbook.
- Morisue, T. (1993). "A comparison of the Coulomb gauge and Lorentz gauge magnetic vector potential formulations for 3D eddy current calculations". In: *IEEE Trans. Magn.* 29.2, pp. 1372–1375.
- Moulder, J.C. and Nakagawa, N (1992). "Characterizing the Performance of Eddy Current Probes Using Photoinductive Field-Mapping". In: *Res Nondestr Eval* 4, pp. 221–236.
- Nakagawa, N. and Beissner, E. (1990). "Probability of Tight Crack Detection via Eddy-Current Inspection". In: *Proceedings of Review of progress in quantitative nondestructive evaluation*. Review of progress in quantitative nondestructive evaluation. Ed. by D.O. Thompson and D.E. Chimenti. Vol. 9A. Plenum Press, pp. 893–899.
- Nakagawa, N., Kubovich, M.W., and Moulder, J.C. (1990). "Modeling Inspectability for an Automated Eddy Current Measurement System". In: *Proceedings of Review of progress in quantitative nondestructive evaluation*. Review of progress in quantitative nondestructive evaluation. Ed. by D.O. Thompson and D.E. Chimenti. Vol. 9A. Plenum Press, pp. 1065–1072.
- Nakata, T. et al. (1990). "Comparison of Different Finite Elements for 3-D Eddy Current Analysis". In: *IEEE Transactions on Magnetics* 26.2, pp. 434–437.
- Nakata, T. et al. (1991). "Comparison of Various Methods of Analysis and Finite Elements in 3-D Magnetic Field Analysis". In: *IEEE Transactions on Magnetics* 27.5, pp. 4073–4076.
- Nath, S., Lord, W., and Rudolphi, T.J. (1993). "Three Dimensional Hybrid Finite-Boundary Element Model for Eddy Current NDE". In: *IEEE Transactions on Magnetics* 29.2, pp. 1853–1856.
- Neighbor, J.E. (1969). "Eddy Current Method for Measuring Anisotropic Resistivity". In: *J. Appl. Phys.* 40, pp. 3078–3080.

- Noritaka, Y. et al. (2006). "Detection of embedded fatigue cracks in Inconel weld overlay and the evaluation of the minimum thickness of the weld overlay using eddy current testing". In: *Nuclear Engineering and Design* 236, 1852–1859.
- Palanisamy, R. and Lord, W. (1979). "Finite Element Modeling of Electromagnetic NDT Phenomena". In: *IEEE Transactions on Magnetics* 15.6, pp. 1479–1481.
- Preis, K., Bíró, O., and Tícar, I. (2000). "Gauged Current Vector Potential and Reentrant Corners in the FEM Analysis of 3D Eddy Currents". In: *IEEE Transactions on Magnetics* 36.4, pp. 418–423.
- Rajesh, S.N., Udpa, L., and Udpa, S.S. (1993). "Numerical Model Based Approach for Estimating POD in NDE Applications". In: *IEEE Transactions on Magnetics* 29 (2), pp. 1857–1858.
- Ren, Z. and Ida, N. (2002). "An artificial neural network for eddy current testing of austenitic stainless steel welds". In: *NDT & E International* 35, pp. 393–398.
- Rosell, A. and Persson, G. (2011). "Modelling a Differential Sensor in Eddy Current Non-destructive Evaluation". In: *Proceedings of the COMSOL Conference*. COMSOL Conference (Stuttgart, Germany). isbn: 978-0-9839688-0-1.
- Rosell, A. and Persson, G. (2012a). "Finite Element Modelling of Closed Cracks in Eddy Current Testing". In: *International Journal of fatigue* 41, pp. 30–38.
- Rosell, A. and Persson, G. (2012b). "Comparison of Experimental and Model Based POD in a Simplified Eddy Current Procedure". In: 18th World Conference on Nondestructive Testing (Durban, South Africa). (Accepted for publication in conference proceedings).
- Rummel, W.D. (1982). "Recommended Practice for Demonstration of Nondestructive Reliability on Aircraft Parts". In: *Materials Evaluation* 40.9, pp. 922–932.
- Shull, P.J. (2002). *Nondestructive evaluation: theory, techniques and applications*. Mechanical engineering 142. New York: Marcel Dekker.
- Singh, R. (2000). *Three Decades of NDI Reliability Assessment*. Report No. Karta-3510-99-01. San Antonio: Karta Technologies inc.
- Song, H. and Ida, N. (1991). "An eddy current constraint formulation for 3d electromagnetic field calculations". In: *IEEE Trans. Magn.* 27.5, pp. 4012–4015.
- Song, S. and Shin, Y. (2000). "Eddy current flaw characterization in tubes by neural networks and finite element modeling". In: *NDT & E International* 33, pp. 233–243.
- Stepinski, T. (2002). "Deep Penetrating Eddy Current for Detection Voids in Copper". In: 8th European Conference on Nondestructive testing (Barcelona, Spain).
- Thompson, R.B. (2001). "Using physical models of the testing process in the determination of Probability of Detection" *Materials Evaluation*". In: *Materials Evaluation* 59.7, pp. 861–865.
- Thompson, R.B. (2007). "A Unified Approach to the Model-Assisted Determination of Probability of Detection". In: *AIP Conf. Proc.* Review of Progress in Quantitative Nondestructive Evaluation (Golden (Colorado)). 975, pp. 1685–1692.
- Uchanin, V. (2001). "New Type multidifferential Eddy Current Probes for Surface and Subsurface Flaw Detection". In: *Zeszyty Problemowe. Badania nieniszczace* Warsaw 6, pp. 201–204.
- Udpa, L. and Udpa, S.S. (1996). "Application of signal processing and pattern recognition techniques to inverse problems in NDE". In: *International Journal of Applied Electromagnetics and Mechanics* 9.1, pp. 1–20.

- Udpa, S.S. and Moore, P.O. (2004). *Electromagnetic testing*. 3rd ed. Vol. 4. Nondestructive testing handbook. American Society for Nondestructive Testing.
- Wall, M. (1997). "Modeling of Inspection Reliability". In: *Engineering Science and Education journal*, pp. 63–72.
- Wanhill, R.J.H. (2002). *Milestone Case Histories in Aircraft Structural integrity*. National Aerospace Laboratory NLR.
- Yee, B.G.W. et al. (1976). *Assessment of NDE Reliability Data*. NASA National Aeronautics and Space Administration CR-134991.
- Zhang, Y., Luo, F., and Sun, H. (2008). "Impedance Evaluation of a Probe-Coil's Lift-off and Tilt Effect in Eddy-Current Nondestructive Inspection by 3D Finite Element Modeling". In: 17th World Conference on Nondestructive Testing (Shanghai, China).